Additional Scalar Bosons in the ATLAS Experiment

Xiaotong Chu
On behalf of the ATLAS Collaboration

13-Sep-2022

中国科学院高能物理研究所
Institute of High Energy Physics
Chinese Academy of Sciences

ATLAS EXPERIMENT

Presented at ICHEP ✓
New results ★

Many Beyond-the-Standard-Model (BSM) models predict extended scalar sectors.

Two-Higgs-Doublet-Models(2HDMs), SuperSymmetry(SUSY),dark matter, axion models… indicate additional scalar or pseudoscalar bosons.

Heavy Neutral Scalar

- $t\bar{t}H/A \to 4top$ ✓
- $t \to qX(\to bb)$ ✓
- $WH(\to WW)$ ✓
- $H \to$ leptons+b-jets ✓
- $A \to ZH(\to bb)$ ✓
- $VH(\to hh)$ ★

Charged Higgs

- ✓ $H^{++}H^{--} \to 4l$
- ★ $H^{\pm} \to ZW \to 3l+\nu$

Light Neutral Scalar

- $X \to \gamma\gamma$ ✓

See Yuan-Tang's talk for SM Higgs decaying to (pseudo)scalar bosons.

Most recent ATLAS results searching for additional scalars with full Run 2 dataset

Heavy Neutral Scalar

* $t\bar{t}H/A \rightarrow t\bar{t}t\bar{t}$

ATLAS-CONF-2022-008

- Search for a **heavy scalar H/A** predicted by 2HDM in $t\bar{t}$ associated production.
  - $H/A \rightarrow t\bar{t}$ dominant decay above 2 top mass.
  - Negative interference effects with SM $gg \rightarrow t\bar{t}$ largely dilute a resonant peak in the $t\bar{t}$ invariant mass spectrum.
- Final states with **same-sign (SS) leptons or ≥3 leptons** and **≥6j (≥2b).**

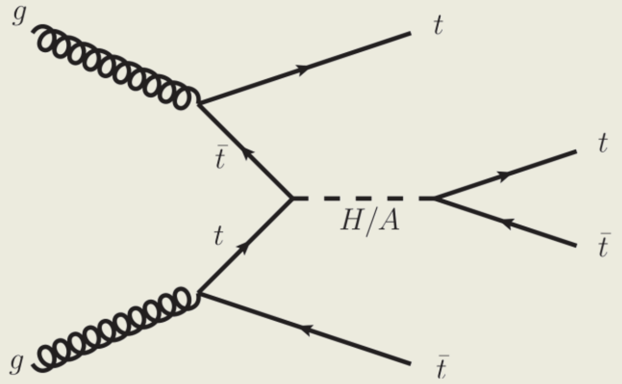

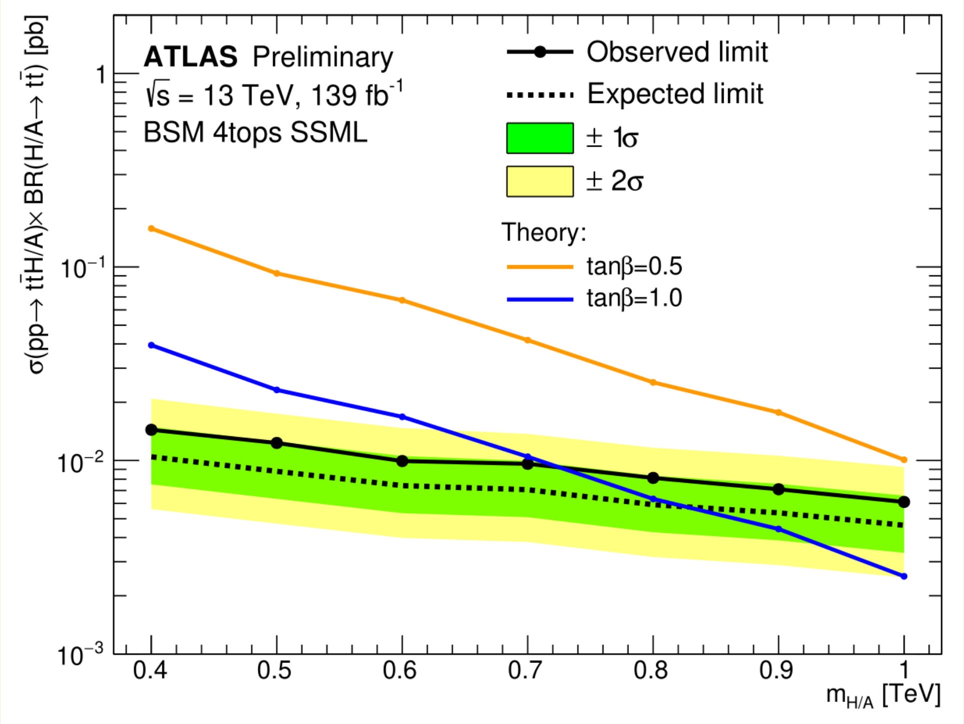

No significant excess of events above the SM prediction is observed.

- Interpretation of the 2HDM type-II for a heavy Higgs mass between 400 and 1000 GeV.
- The best fitted value is **compatible** with previous ATLAS $t\bar{t}t\bar{t}$ cross-section measurement (EPJC 80 (2020) 1085).

FCNC t→qX(→ bb)

ATLAS-CONF-2022-027

- Non-SM Higgs field ***X (flavon)*** with flavour charge.
  - Predicted by Froggatt-Nielsen mechanism to probe **Flavour-changing neutral-current (FCNC) couplings** with first and second generation quarks.
  - For a neutral scalar particle below 200 GeV the leading decay mode is $\boldsymbol{X \rightarrow b\bar{b}}$.
- Generic search by **top-quark pair production**:
  - One top quark decays to X ($\boldsymbol{m_X < m_{top}}$) and up-type quark ($u/c$).
  - The other top quark decays to Wb.

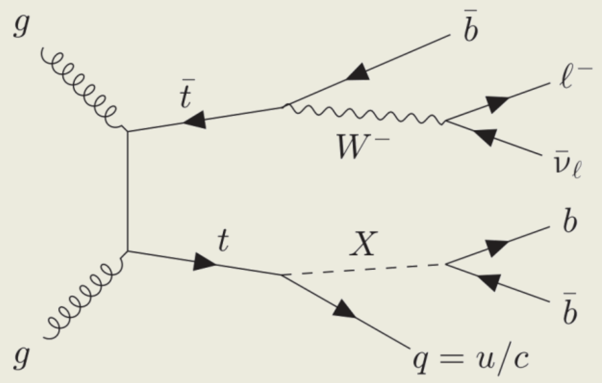

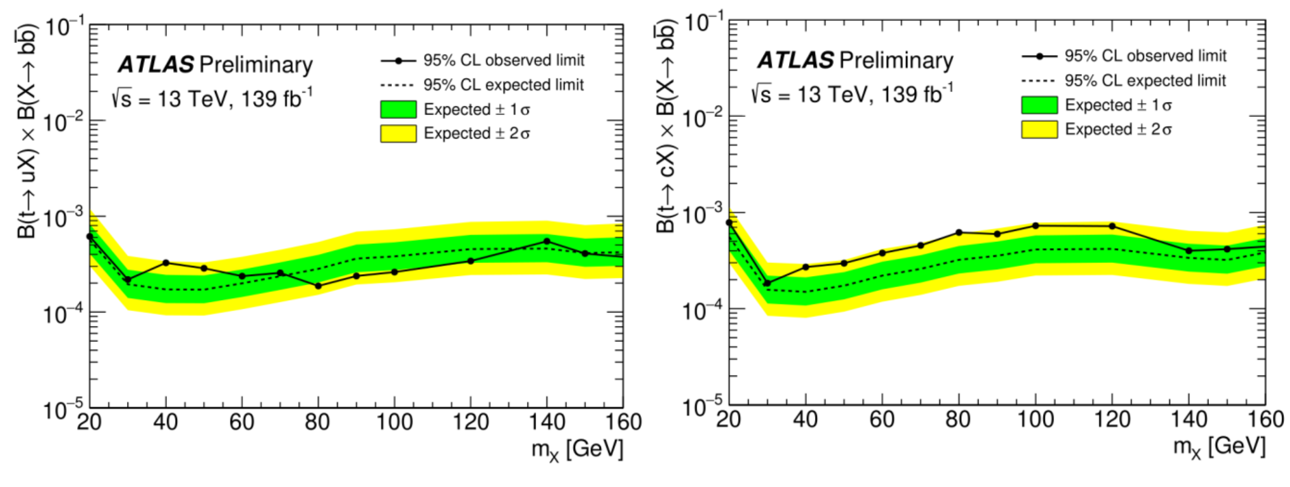

(a) $t \rightarrow uX$ (b) $t \rightarrow cX$

No significant excess is observed.

- Slight excess (1.8σ) at 40 GeV in $t \rightarrow uX$ channel and ~2σ broad excess in $t \rightarrow cX$ channel.
- Expected limits ~**a factor of three better** than the previous ATLAS results (FCNC t→qH, JHEP 05 (2019) 123) scaled to the same integrated luminosity.

WH(→WW)

ATLAS-CONF-2022-033

- Generic search utilizing a general effective Lagrangian including dimension six operators in effective field theory.
- Associated production of **heavy scalar (H) with W boson** in $l^{\pm}\nu l^{\pm}\nu\ qq$ final state.
  - Complementary to gluon-gluon fusion (ggF) and vector boson fusion (VBF) searches.
  - Larger cross sections than VBF production and smaller background.
- Two signal regions (SR) with two same-sign(SS) leptons and two WZ control regions, depending on the reconstruction of W→qq decay:
  - **Resolved**: two small radius jets.
  - **Boosted**: one large radius jet.

No significant excess is observed.

- Upper limits on the heavy Higgs boson production cross-section as a function of the **heavy Higgs boson mass** and the **two BSM HVV coupling strengths** $\frac{\rho_H f_W}{\Lambda^2}$, $\frac{\rho_H f_{WW}}{\Lambda^2}$.

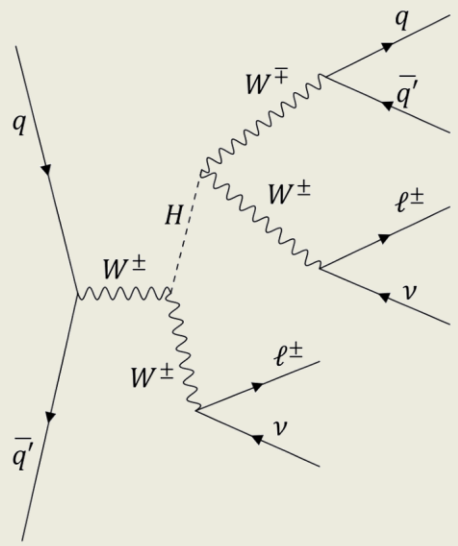

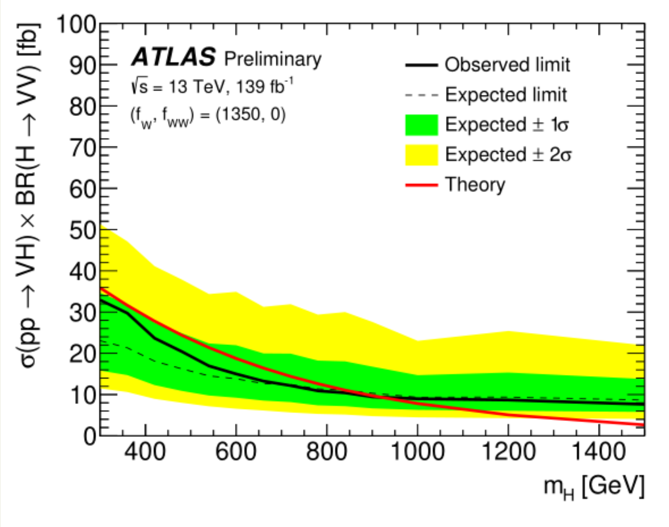

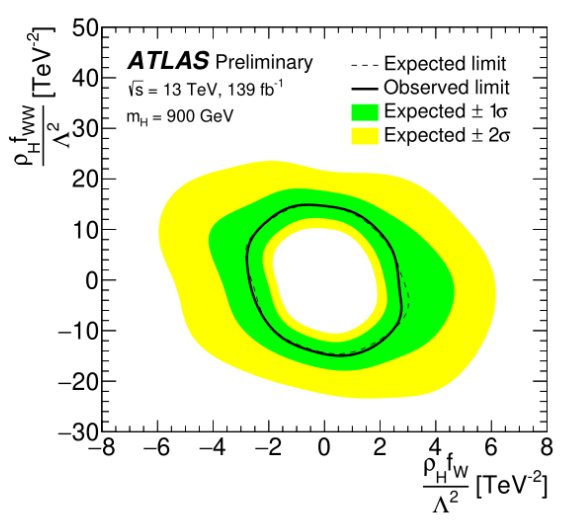

Flavour-violating H→leptons+b-jets

[ATLAS-CONF-2022-039]

- General two Higgs doublet model (**g2HDM**) without Z_2 symmetry, featuring FCNH (Flavour Changing Neutral Higgs) couplings.
  - Couplings of H involving top-quark: ρ_{tt}, ρ_{tc}, and ρ_{tu}.
- First analysis to target BSM production leading to three-top final states and the first to probe g2HDM.
- Sensitive probe of new physics: **same-sign (SS) top, 3-top, 4-top** final states.

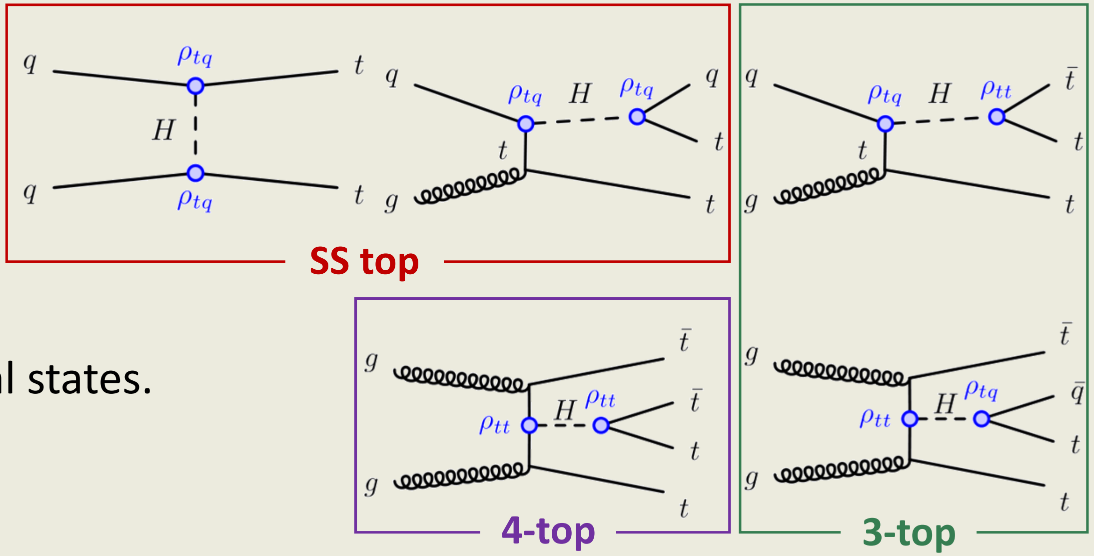

$m_H = 1000$ GeV
$\rho_{tt} = 0.32$
$\rho_{tc} = 0.05$
$\rho_{tu} = 0.85$

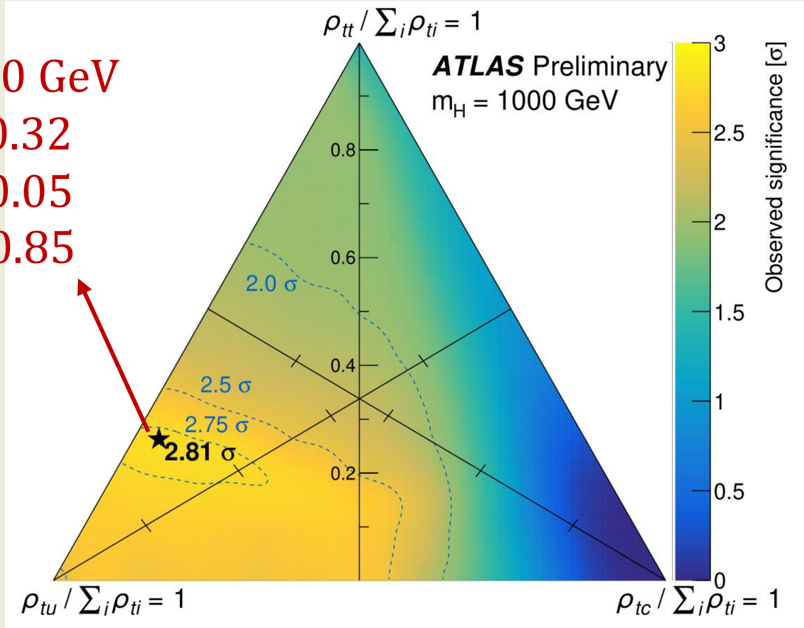

No significant excess over SM background is observed.

- Most significant deviation observed at **m_H=1000 GeV** with **local significance of 2.81 σ**.
- Results are also interpreted in RPV SUSY model.

$A \to Zh(\to b\bar{b})$

arXiv:2207.00230

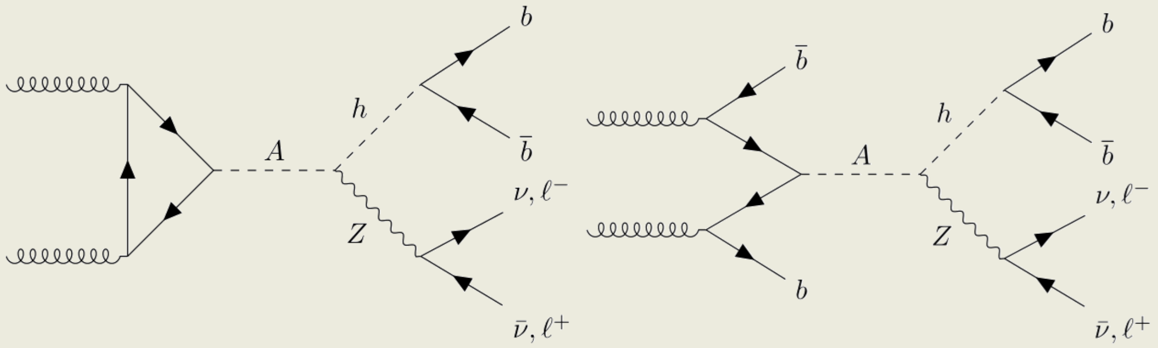

- Search for **heavy pseudoscalar A** decaying to Z boson and SM Higgs in ggF or b-associated production.
- Signal regions categorized according to **0ℓ ($Z \to \nu\nu$)** or **2ℓ ($Z \to ll$)** and b-jet multiplicity.
- Model-independent limits on ggA and bbA (combined 0ℓ+2ℓ).
  - Largest deviation from the SM expectation found at **500 GeV** in ggA search, corresponding to significance of **2.1σ (1.1 σ) local (global)** (1.6 σ for bbA).
- Interpretation for four 2HDM types.

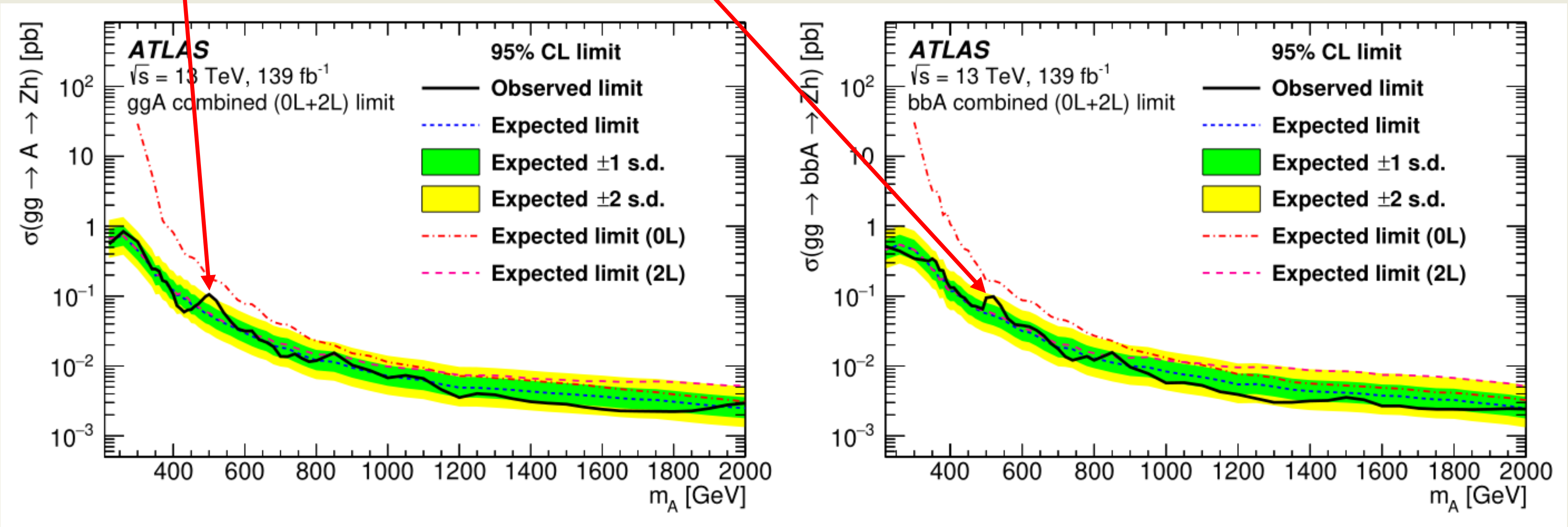

No significant excess is observed.

VH(→hh)

ATLAS-CONF-2022-043

- **Neutral heavy CP-even scalar H→hh→bbbb** in association with a vector boson (W or Z).

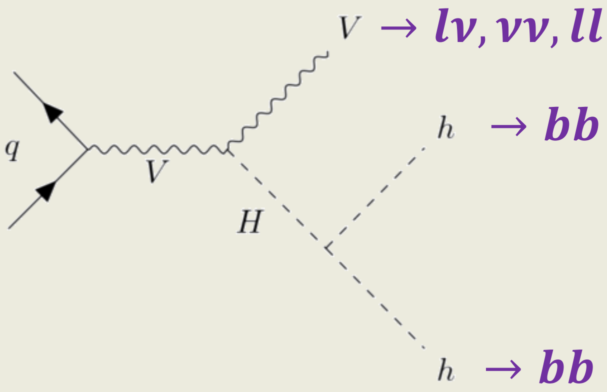

SM-like non-resonant hh production

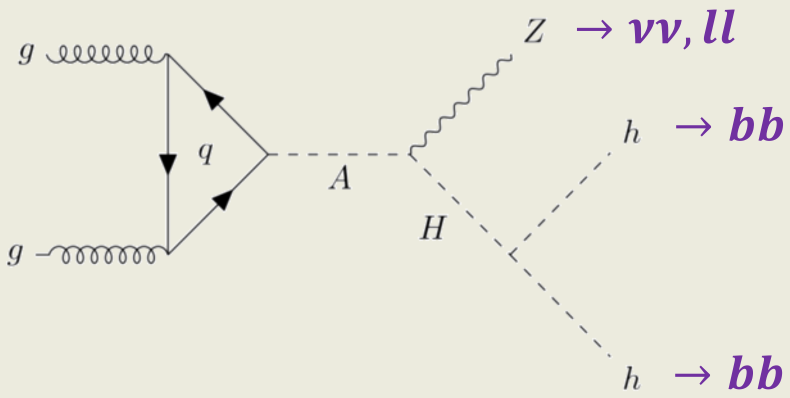

Decay of a neutral heavy pseudoscalar A

- **Three leptonic channels (0L, 1L, 2L)** define the signal regions.
- m_{hh} / m_{Zhh} mass resolution improved by **scaling the b-jet momenta** with the ratio of the measured di-b-jet mass to 125 GeV.
  - The relative m_{hh} resolution **improves by a factor of ~3**.

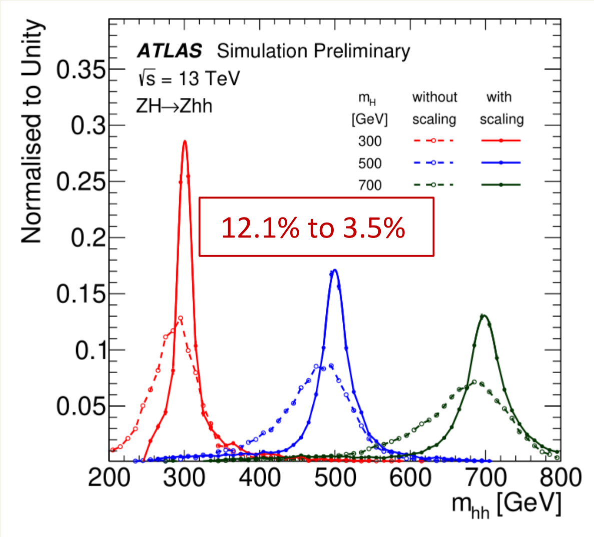

VH(→hh)

ATLAS-CONF-2022-043

- Multivariate techniques based on boosted decision trees (BDT) are used as final discriminants to extract potential signal contributions.
- Maximum-likelihood fit to BDT distributions in the SRs to extract the results.

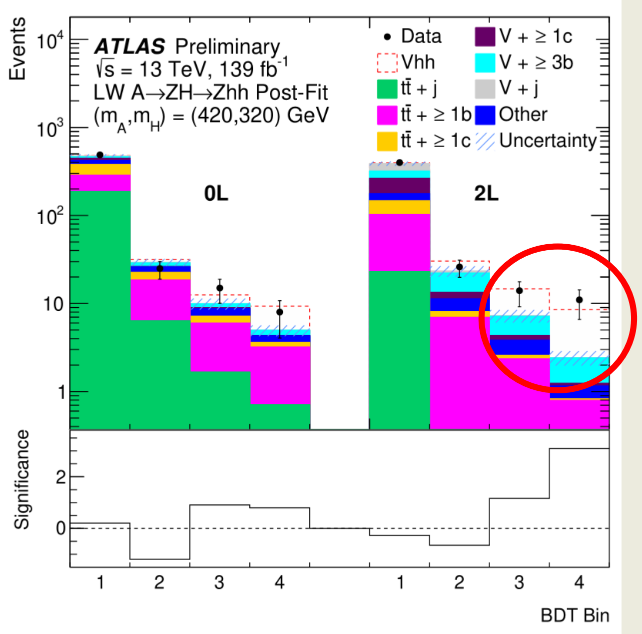

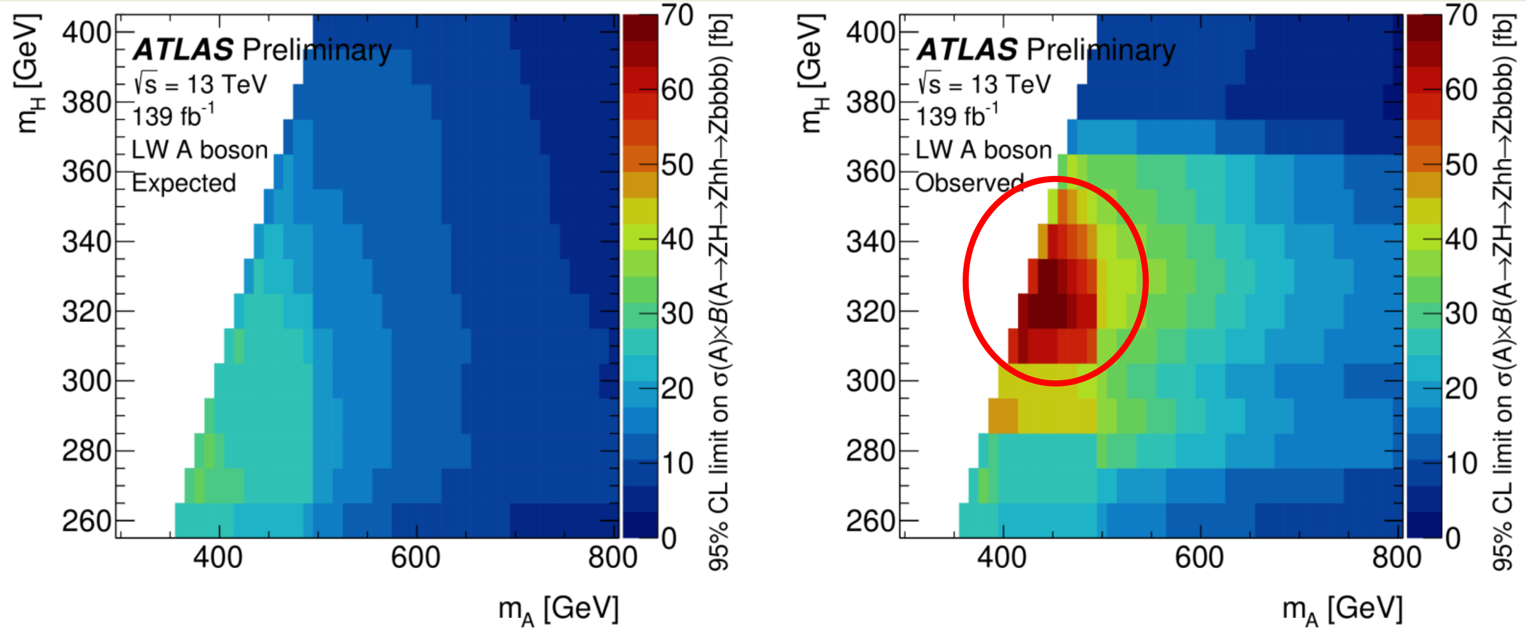

- **Large-width LW A→ZH channel (m_A, m_H) = (420, 320) GeV** with local (global) significance of **3.8σ (2.8σ)**.
- The upper limits are calculated for type-I 2HDM and for the lepton-specific 2HDM.

Light Neutral Scalar

Low mass $X \rightarrow \gamma\gamma$

ATLAS-CONF-2022-018

- Search for **di-photon resonances** in the **mass range between 10 to 70 GeV**.
- Exploit the particular kinematics of events to **reach invariant masses down to 10 GeV**.
  - Select close-by γγ pairs (boosted against a jet) and $p_T^{\gamma\gamma}$ > 50 GeV to overcome trigger energy threshold.
  - Complex analytic function used to adequately model low-mass turn-on and inflection feature.
- Most significant deviation from the background observed at **19.4 GeV** with **local (global) significance 3.05σ (1.48σ).**
- The observed limits are recasted in the parameter space of an axion-like particle, covering a longstanding gap in di-photon resonance searches.

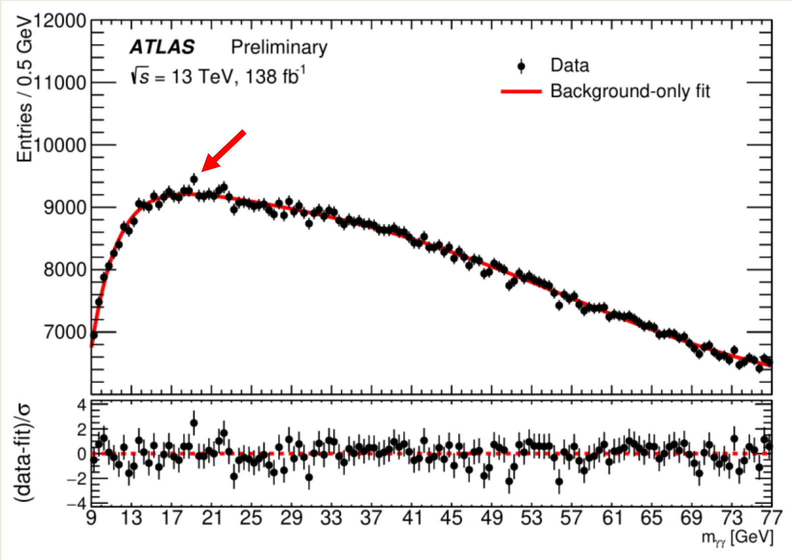

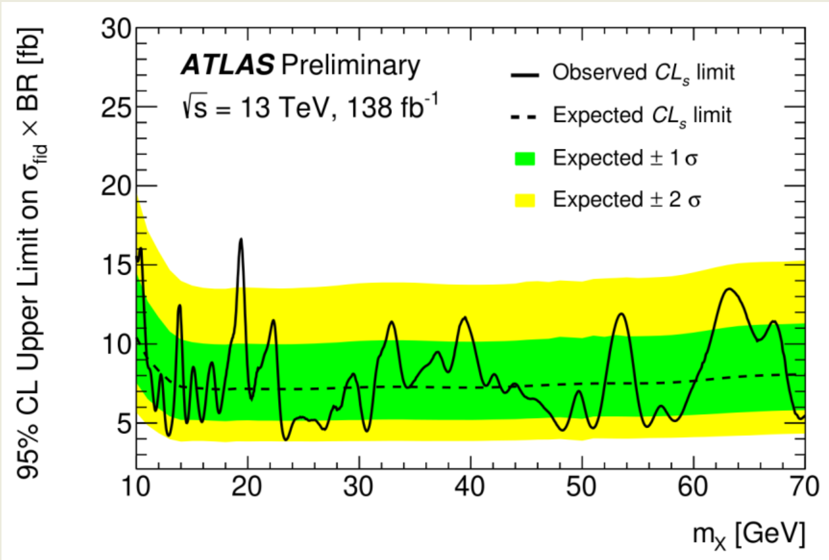

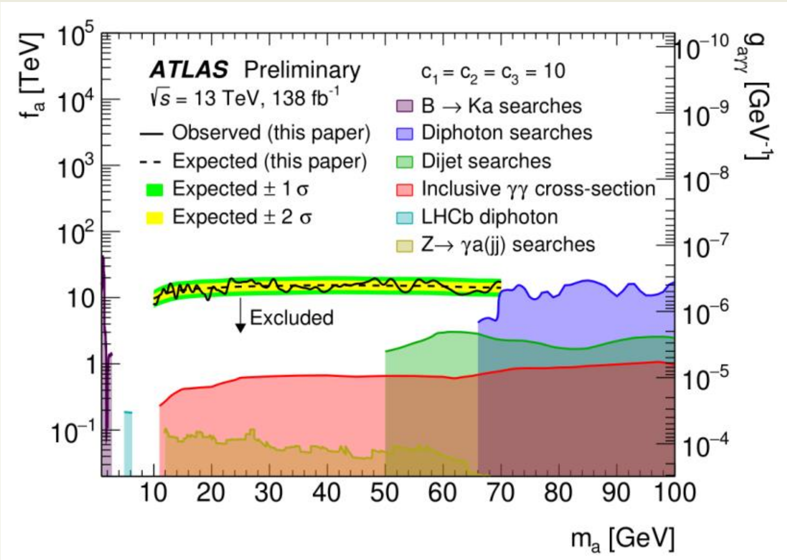

Charged Higgs Boson

$H^{++}H^{--} \rightarrow 4l$

ATLAS-CONF-2022-010

- Searches for **doubly charged Higgs boson** $H^{\pm\pm} \rightarrow l^{\pm}l'^{\pm}$ (l, l' = e, μ, leptonic τ) pair decays.
  - Left-right symmetric (LRS) models, Georgi-Machacek model…
  - Lepton flavor violation (LFV) decays are allowed: $H^{\pm\pm} \rightarrow l^{\pm}l'^{\pm}$.
    - Couplings assumed to be the same for all flavor combinations.

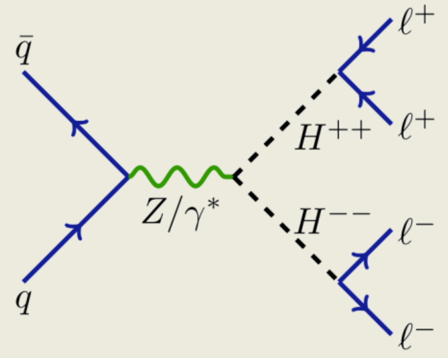

No significant excess over SM prediction is observed.

- Combined lower limit on $H^{\pm\pm}$ mass at **1080 GeV** under the assumption $\sum_{ll'} B(H^{\pm\pm} \rightarrow l^{\pm}l'^{\pm}) = 100\%$.
  - 300 GeV higher than the previous ATLAS measurement (Eur. Phys. J. C 78 (2018) 199).

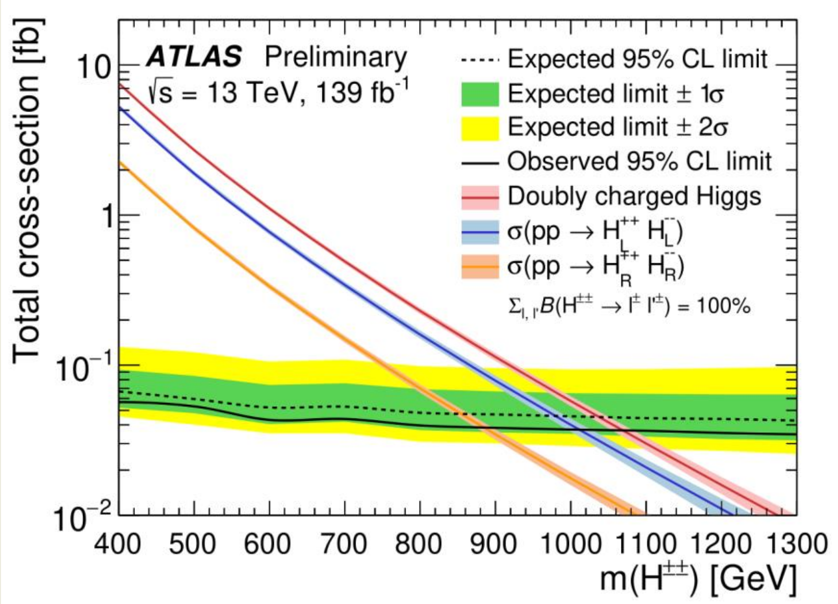

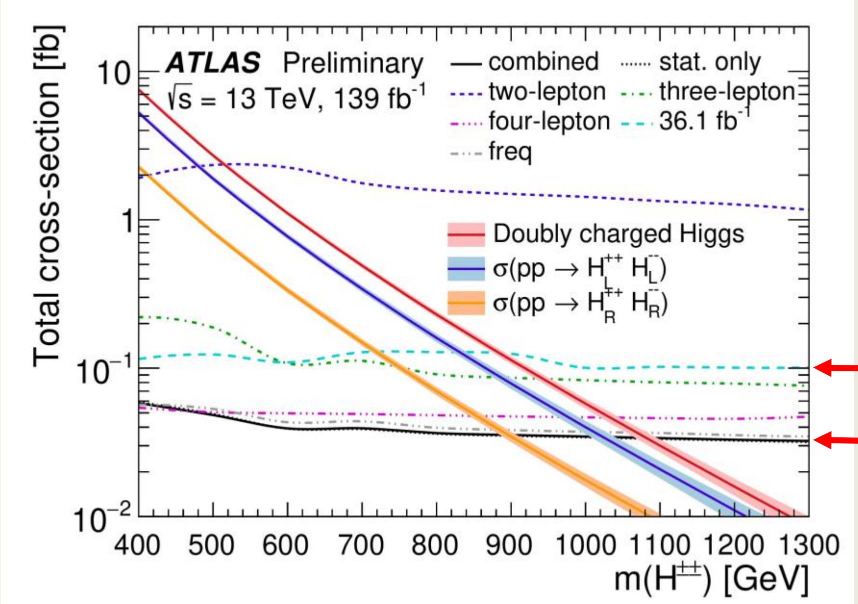

* $H^{\pm} \rightarrow ZW \rightarrow l\nu l'l'$

arXiv:2207.03925

- Search for WZ **resonance** in fully leptonic final state.
  - Heavy Vector Triplet (HVT) model as benchmark for W' and **Georgi–Machacek model for $H_5^{\pm}$**.
  - The **fully leptonic channel is more sensitive** to resonances with mass below ~ 1 TeV because of the low background, in spite of the low branching ratio.

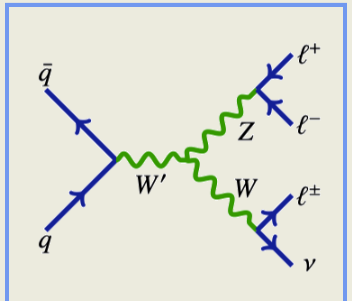

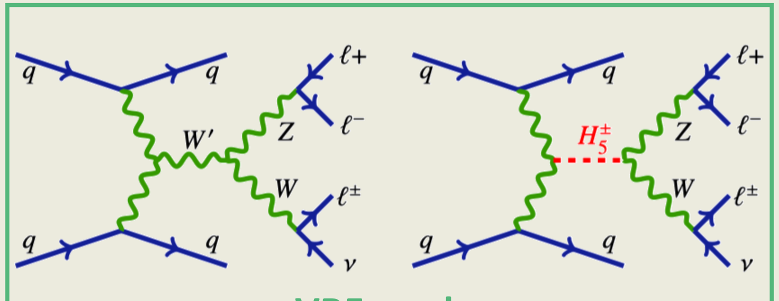

- All final states with three charged leptons (e or μ) and missing transverse momentum from WZ leptonic decays are considered.
- Two selections are defined in order to build signal regions targeting Drell–Yan and VBF productions modes.
  - **Drell-Yan SR**: cut-based selection.
  - **VBF SR**: Artificial neural network (ANN).

Training variable
m_{jj}
$\Delta\phi_{jj}$
η_W, η_Z
η_{j1}
ζ_{Lep}
$E_{\mathrm{T}}^{\mathrm{miss}}$
H_{T}

$H^{\pm} \to ZW \to l\nu l'l'$

arXiv:2207.03925

- Simultaneous maximum-likelihood fit of binned m(WZ) in SR & CRs are performed.
  - Local (global) significance of **2.8σ (1.6σ) at 375 GeV** in **VBF SR.**
- Observed and expected exclusion limits at 95% CL on $\sigma \times B(H_5^{\pm} \to WZ)$ and on the mixing parameter $sin\theta_H$.
  - Exclusion limits of $sin\theta_H$ are **~35% stronger** than previous ATLAS result (Phys. Lett. B 787 (2018) 68).
- Upper limits are also set on HVT $W' \to WZ$ in the Drell–Yan and VBF SRs separately. (See backup slides.)

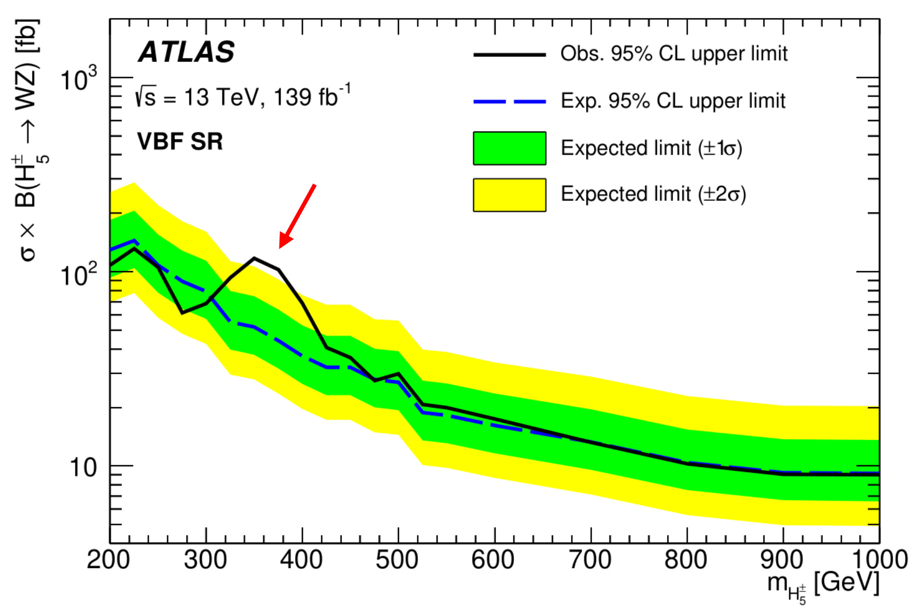

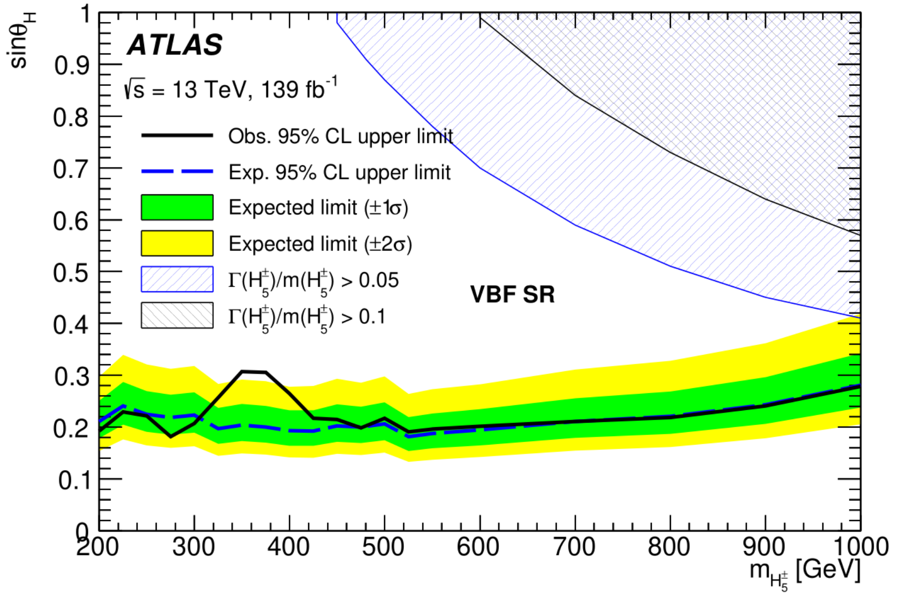

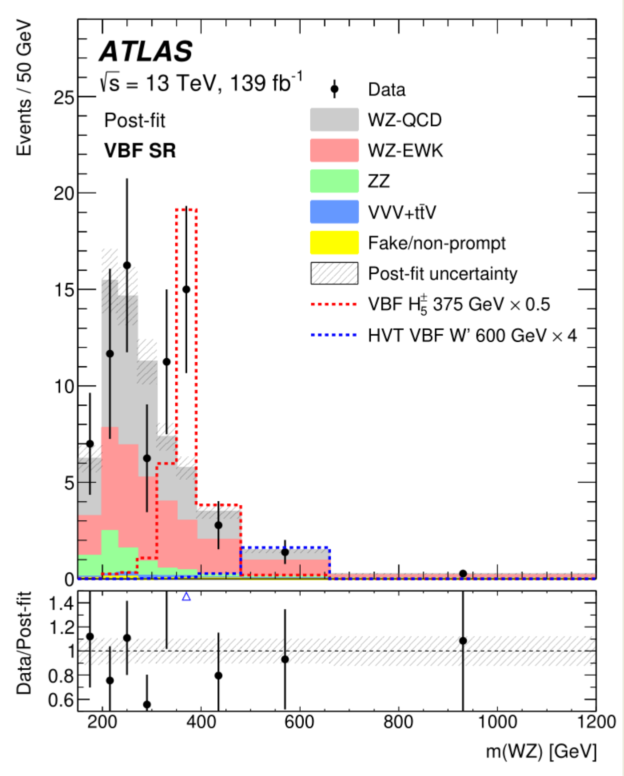

Summary plots for hMSSM interpretations

ATL-PHYS-PUB-2022-043

Newly added | Updated

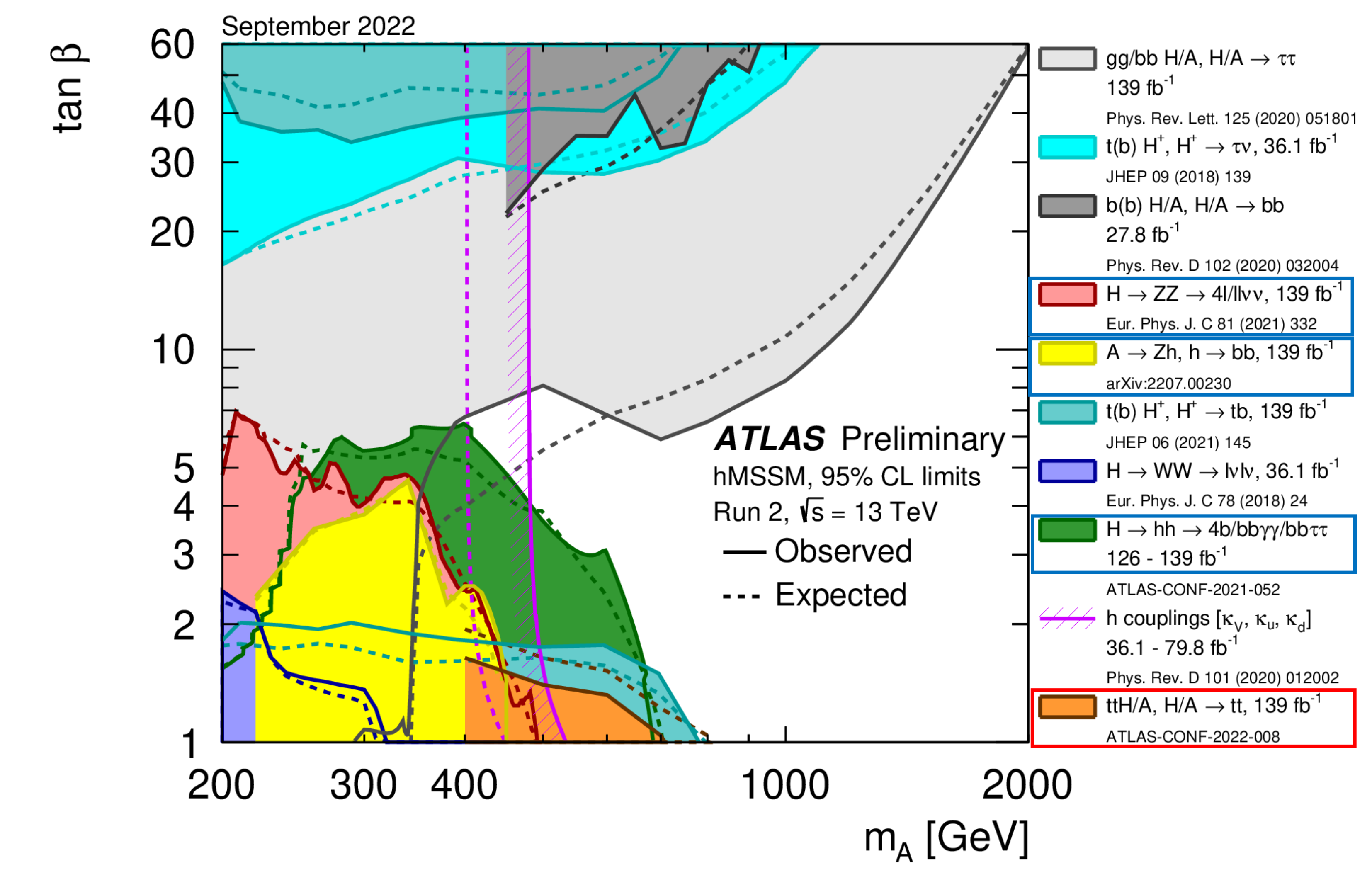

- Benchmark scenario for the Minimal Supersymmetric Standard Model (MSSM) Higgs sector.
- Unless otherwise specified, only gluon–gluon fusion is considered for the production mode.

Summary plots for Type-I 2HDM interpretations

ATL-PHYS-PUB-2022-043

- Benchmark scenario of type-I 2HDM with assumptions: $\mathrm{m_H} = m_A = \mathrm{m_{H^\pm}}, \mathrm{m_h} = 125\ \mathrm{GeV}, m_{12}^2 = m_A^2$.
- Assume a narrow width (< 5%) Higgs boson.

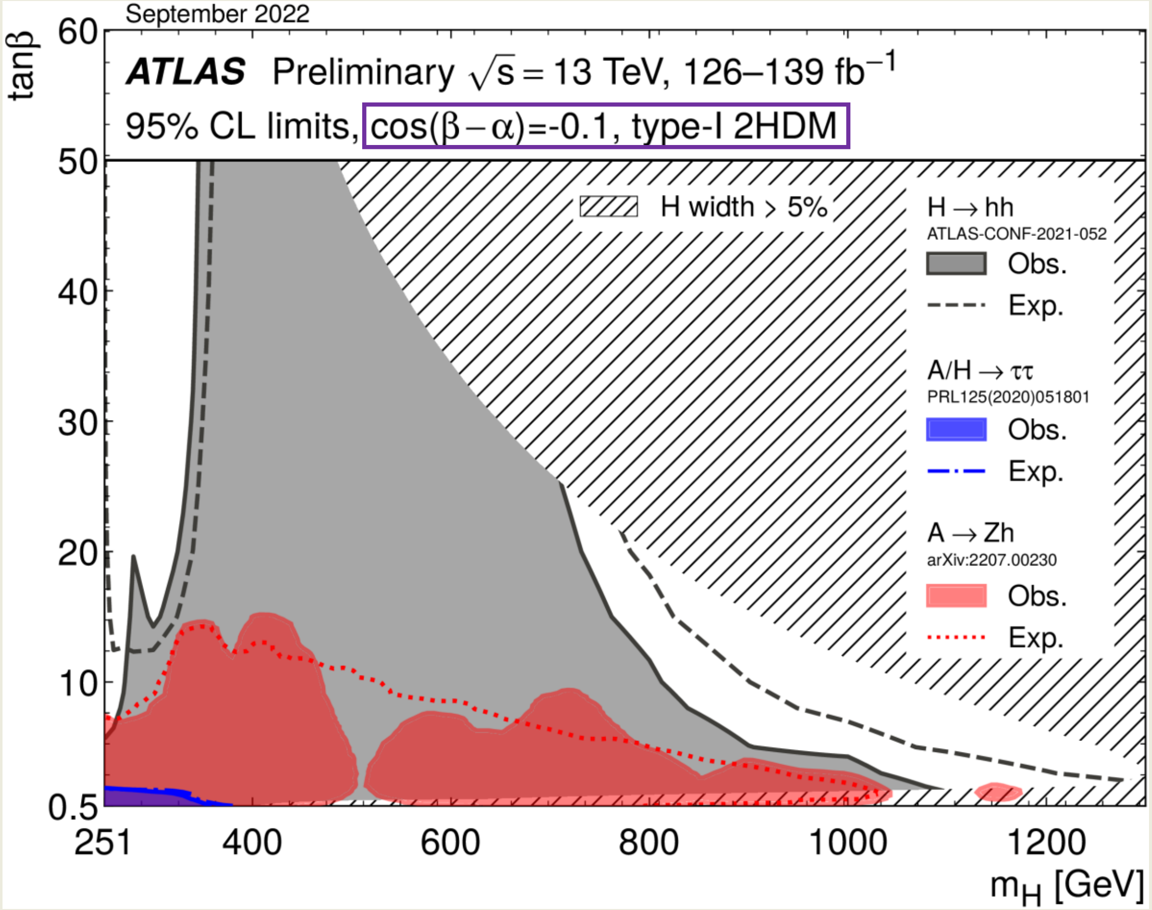

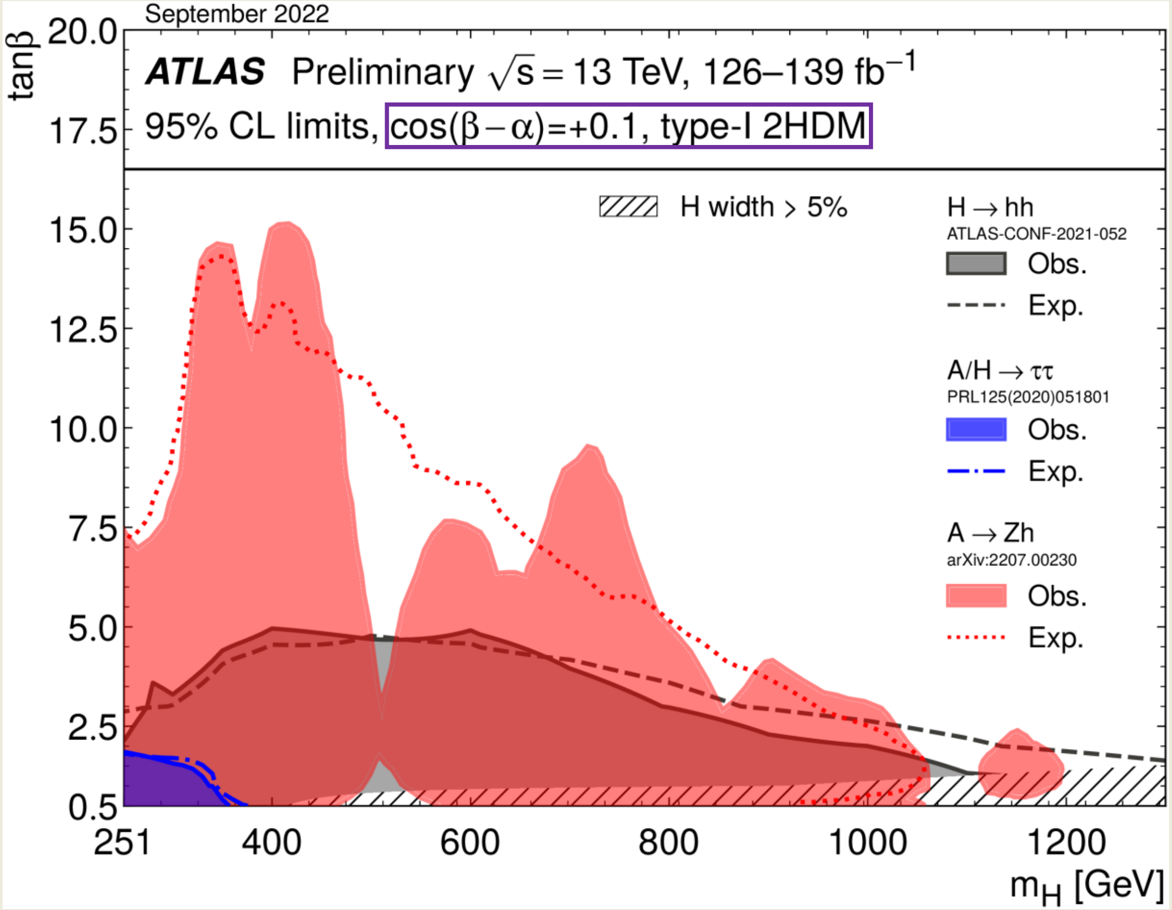

Summary

- Comprehensive programs from the ATLAS experiment targeting signatures of additional scalars and pseudoscalars.
- Results are generally consistent with the Standard Model expectations.
- More results with full Run 2 data are still being released.
- Looking forward to uncovering more of the phase space in Run-3!

THANK YOU!

$t\bar{t}H/A \rightarrow t\bar{t}t\bar{t}$

ATLAS-CONF-2022-008

- Two BDT classifiers are used:

SM BDT:

Separates SM $t\bar{t}t\bar{t}$ events from other SM backgrounds due to the similar kinematics of the signal and SM $t\bar{t}t\bar{t}$ events.

BSM pBDT (BSM mass-parametrised BDT):

Discriminates BSM $t\bar{t}t\bar{t}$ signal events against all backgrounds.

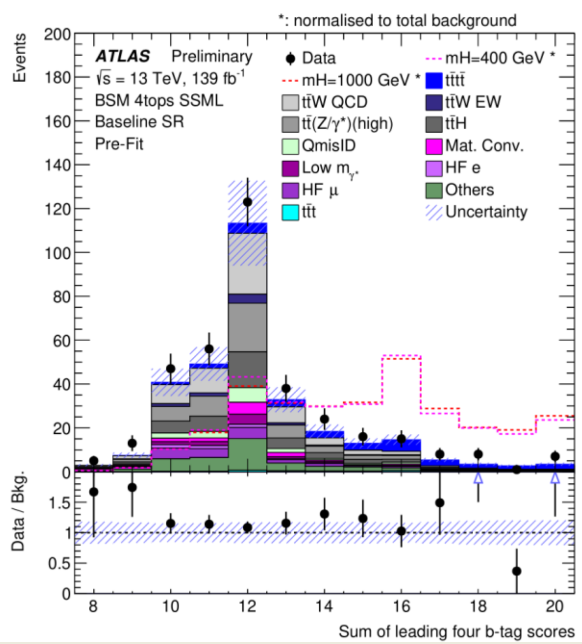

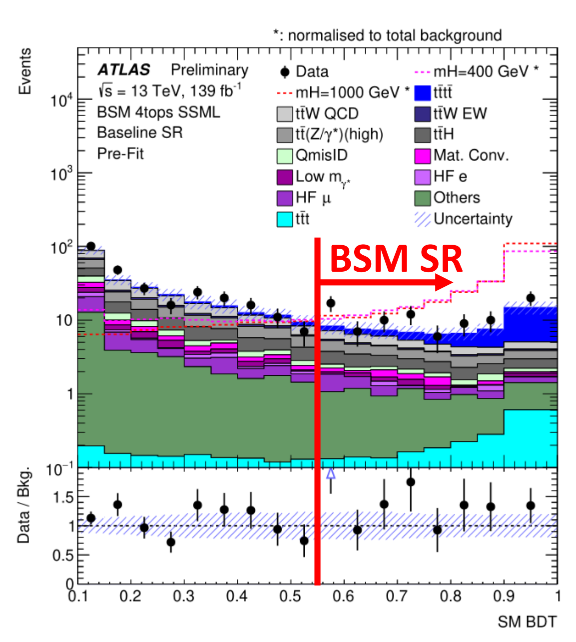

Process	Pre-fit	Post-fit
$t\bar{t}t\bar{t}$	22.3 ± 5.4	25.9 ± 5.4
$t\bar{t}W$ QCD	9.4 ± 9.3	17.1 ± 6.9
$t\bar{t}W$ EW	1.3 ± 0.5	1.4 ± 0.6
$t\bar{t}WW$	1.8 ± 1.0	1.9 ± 1.0
$t\bar{t}(Z/\gamma^*)$ (high mass)	8.5 ± 2.2	9.2 ± 2.3
$t\bar{t}H$	7.2 ± 1.7	7.8 ± 1.7
QmisID	2.1 ± 0.1	2.1 ± 0.1
Mat. Conv.	1.8 ± 0.6	3.0 ± 1.2
Low m_{γ^*}	1.2 ± 0.6	0.8 ± 0.8
HF e	0.6 ± 0.5	0.6 ± 0.5
HF μ	2.7 ± 1.0	2.9 ± 1.2
LF	1.1 ± 1.2	0.4 ± 1.0
Other fake	1.1 ± 0.7	1.3 ± 0.7
tZ, tWZ	0.9 ± 0.3	0.9 ± 0.3
VV, VH, VVV	0.3 ± 0.1	0.3 ± 0.1
$t\bar{t}t$	1.9 ± 1.9	2.3 ± 2.1
$t\bar{t}WZ$, $t\bar{t}ZZ$, $t\bar{t}WH$, $t\bar{t}HH$	1.3 ± 0.3	1.4 ± 0.3
Total background	65.6 ± 13.2	79.5 ± 6.8
$t\bar{t}H(\rightarrow t\bar{t})$, m_H = 400 GeV	38.6 ± 2.4	–
$t\bar{t}H(\rightarrow t\bar{t})$, m_H = 1000 GeV	4.4 ± 0.2	–
Data	91	

* $t\bar{t}H/A \rightarrow t\bar{t}t\bar{t}$

ATLAS-CONF-2022-008

- Uncertainties associated to the generator are estimated by comparing the prediction from the nominal samples with the alternative samples generated with Madgraph5_aMC@NLO. The uncertainties due to missing higher-order QCD corrections are evaluated in the same way as for the signal.
- 12% (10%) on $t\bar{t}Z$ ($t\bar{t}H$) total cross-section.
- 1% to both $t\bar{t}Z$ and $t\bar{t}H$.
- 20% to $t\bar{t}W$ EW cross-section. Additional 124% (200%) to $t\bar{t}W$ QCD production with seven (eight or more) jets.
- 50% to events with an additional true b-jet and a separate 50% uncertainty to events with additional two or more true b-jets.
- Uncertainty on $t\bar{t}t$ cross-section is set to 100%.
- An extra uncertainty of 50% to $t\bar{t}t$ with at least one additional true b-jet.
- 30% to the cross-section of tZ and tWZ single-top-quark processes.
- Uncertainty on diboson cross-section is set to 40%.
- For rare top-quark processes, $t\bar{t}WW$, $t\bar{t}ZZ$, $t\bar{t}WZ$, $t\bar{t}HH$, $t\bar{t}WH$, an uncertainty on the cross-section of 50%.
- For the remaining small backgrounds, an uncertainty of 50% is assigned to the cross-section.
- An additional uncertainty of 50% is applied to all small backgrounds except $t\bar{t}t$.
- 50% (100%) for the material conversion background applied to events with mCV ee > 0.1 GeV.
- Uncertainty of normalisation of the background coming from light-flavour non-prompt leptons is 100%.
- 30% for fakes/non-prompt leptons.
- Uncertainty of 30% is assigned to events with three true b-jets, and a separate 30% uncertainty to events with at least four true b-jets.

* $t\bar{t}H/A \rightarrow t\bar{t}t\bar{t}$

ATLAS-CONF-2022-008

Region	Channel	N_j	N_b	Other selection cuts	Fitted variable
CR Conv	$e^{\pm}e^{\pm} \mid\mid e^{\pm}\mu^{\pm}$	$4 \leq N_j < 6$	≥ 1	$m_{ee}^{CV} \in [0, 0.1]$ GeV $200 < H_T < 500$ GeV	m_{ee}^{PV}
CR HF e	$eee \mid\mid ee\mu$		$= 1$	$100 < H_T < 250$ GeV	Yield
CR HF μ	$e\mu\mu \mid\mid \mu\mu\mu$		$= 1$	$100 < H_T < 250$ GeV	Yield
CR $t\bar{t}W$	$e^{\pm}\mu^{\pm} \mid\mid \mu^{\pm}\mu^{\pm}$	≥ 4	≥ 2	$m_{ee}^{CV} \notin [0, 0.1]$ GeV, $\lvert\eta(e)\rvert < 1.5$ for $N_b = 2$, $H_T < 500$ GeV or $N_j < 6$; for $N_b \geq 3$, $H_T < 500$ GeV	$\sum p_T^{\ell}$
CR lowBDT	SS+3L	≥ 6	≥ 2	$H_T > 500$ GeV, SM BDT < 0.55	SM BDT
BSM SR	SS+3L	≥ 6	≥ 2	$H_T > 500$ GeV, SM BDT $\geq$ 0.55	BSM pBDT

SM BDT

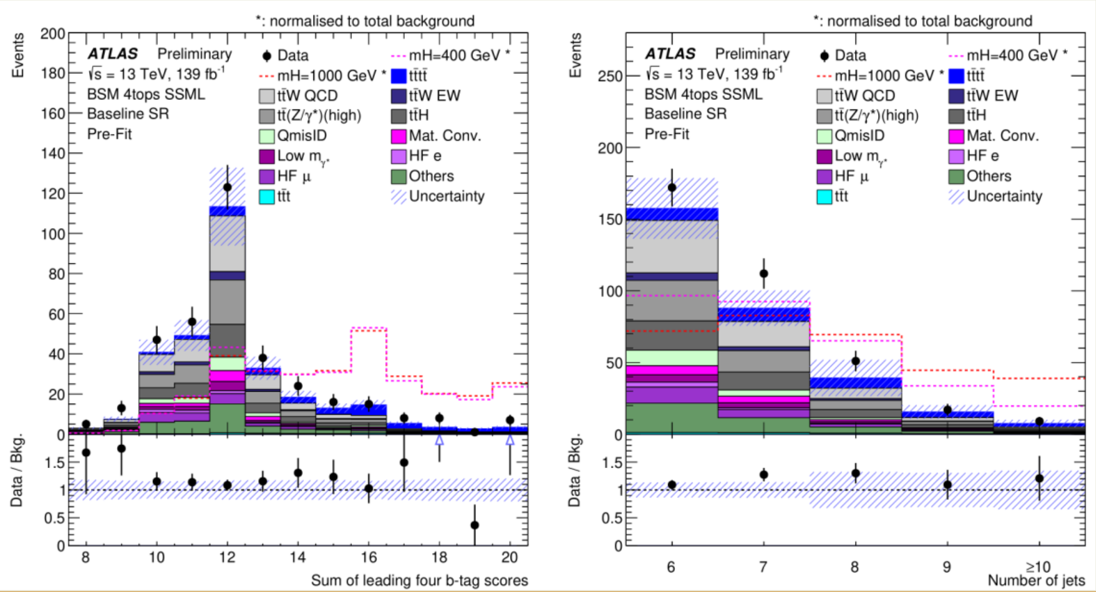

BSM pBDT

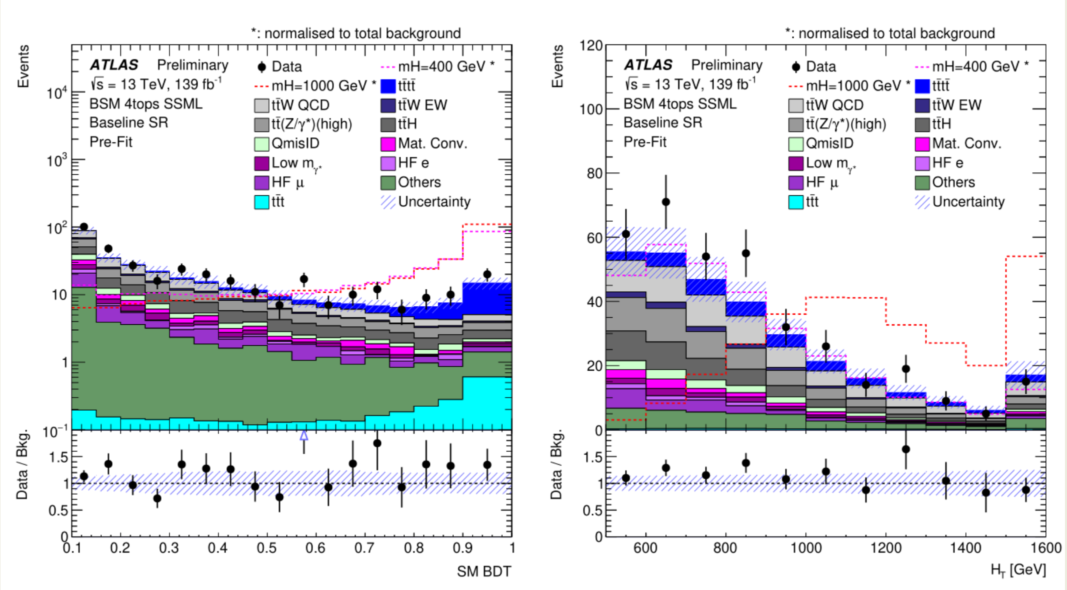

$t\bar{t}H/A \rightarrow t\bar{t}t\bar{t}$

ATLAS-CONF-2022-008

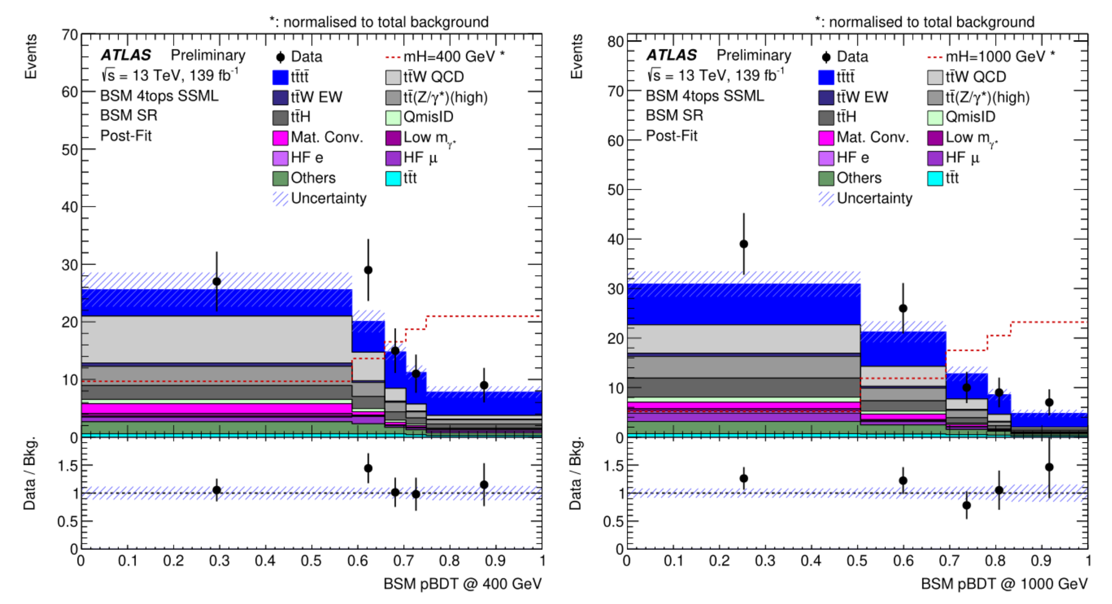

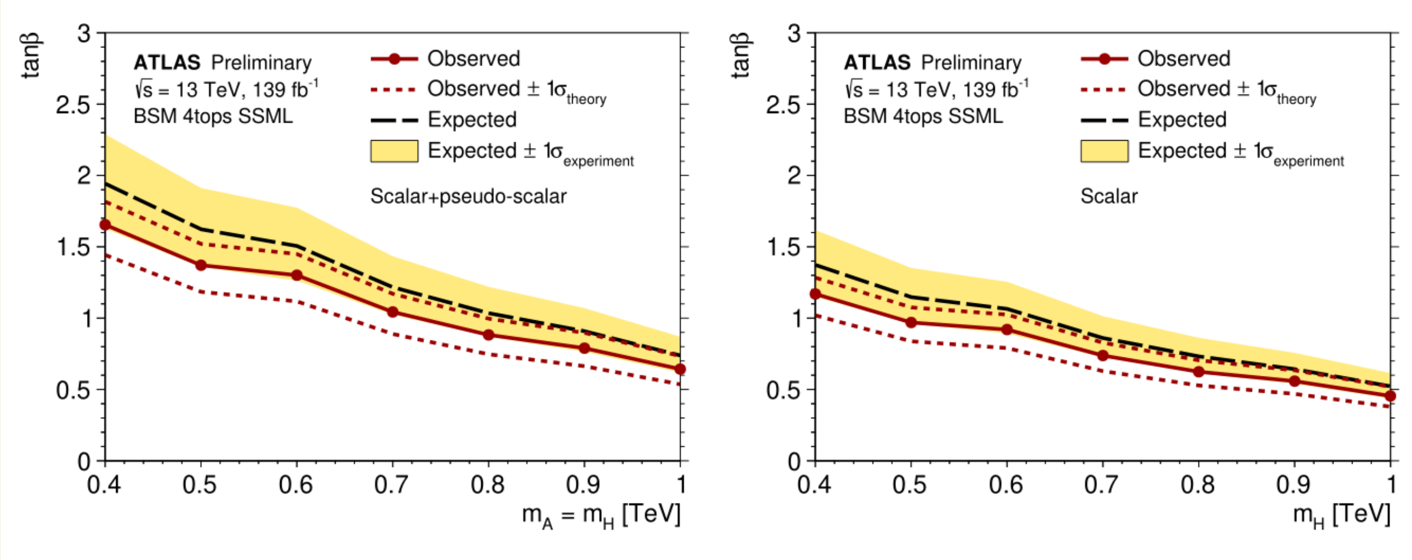

FCNC t→qX(→ bb)

ATLAS-CONF-2022-027

- Signal and control regions are defined based on jet and b-jet multiplicity: SR 4j 3b, 5j 3b, 6j 3b; CR 4j 4b, 5j ≥4b, 6j ≥4b.
- A discriminant Neural Network (NN) is trained for each $t \to uX$ or $t \to cX$ process to distinguish signal and background.

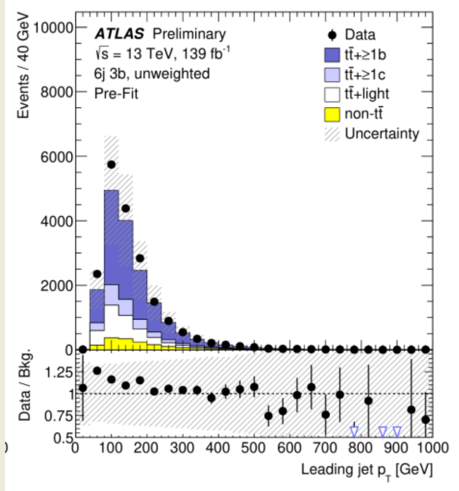

Reweight

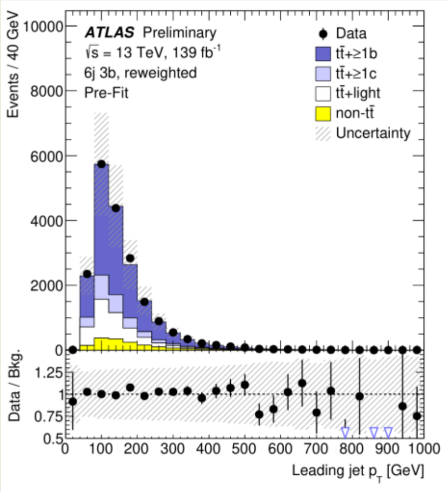

- Reweight using $\boldsymbol{H_T^{all}}$, the scalar sum of the transverse momenta of all selected objects in the event to correct mismodelling of MC predictions.

$$R(H_{\mathrm{T}}^{\mathrm{all}}) = \frac{N_{\mathrm{Data}}(H_{\mathrm{T}}^{\mathrm{all}}) - N_{\mathrm{MC}}^{\text{non-}t\bar{t}}(H_{\mathrm{T}}^{\mathrm{all}})}{N_{\mathrm{MC}}^{t\bar{t}}(H_{\mathrm{T}}^{\mathrm{all}})}$$

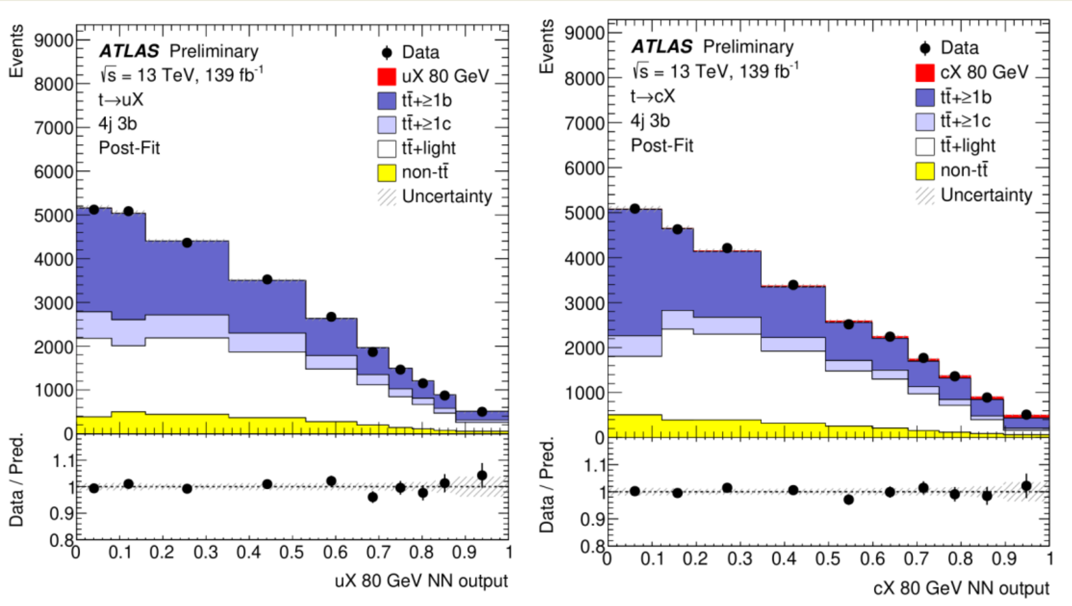

FCNC t→qX(→ bb)

ATLAS-CONF-2022-027

Uncertainty source	$\Delta\mu(uX_{30})$	$\Delta\mu(uX_{80})$	$\Delta\mu(uX_{120})$
$t\bar{t}$+≥1b modelling	0.040	0.060	0.098
$t\bar{t}$+≥1c modelling	0.033	0.055	0.091
$t\bar{t}$+light modelling	0.034	0.058	0.040
$t\bar{t}$+≥1b normalisation	0.012	0.011	0.039
$t\bar{t}$+≥1c normalisation	0.017	0.036	0.087
$W \to cb$ modelling	0.001	0.010	0.017
Reweighting	0.005	0.013	0.017
Other backgrounds	0.008	0.026	0.023
Luminosity, JVT, pile-up	0.002	0.006	0.012
Lepton trigger, identification, isolation	0.001	0.004	0.007
Jet energy scale and resolution	0.008	0.037	0.040
b-tagging efficiency for b-jets	0.007	0.008	0.041
b-tagging efficiency for c-jets	0.014	0.027	0.079
b-tagging efficiency for light jets	0.007	0.008	0.010
$E_{\mathrm{T}}^{\mathrm{miss}}$	0.002	0.010	0.011
Total systematic uncertainty	0.077	0.125	0.220
Signal statistical uncertainty	0.014	0.009	0.007
Total statistical uncertainty	0.064	0.070	0.065
Total uncertainty	0.098	0.141	0.230

Uncertainty source	$\Delta\mu(cX_{30})$	$\Delta\mu(cX_{80})$	$\Delta\mu(cX_{120})$
$t\bar{t}$+≥1b modelling	0.034	0.074	0.079
$t\bar{t}$+≥1c modelling	0.010	0.012	0.040
$t\bar{t}$+light modelling	0.008	0.049	0.038
$t\bar{t}$+≥1b normalisation	0.026	0.038	0.001
$t\bar{t}$+≥1c normalisation	0.019	0.048	0.013
$W \to cb$ modelling	0.001	0.020	0.015
Reweighting	0.005	0.013	0.019
Other backgrounds	0.009	0.057	0.047
Luminosity, JVT, pile-up	0.005	0.005	0.003
Lepton trigger, identification, isolation	0.001	0.004	0.003
Jet energy scale and resolution	0.017	0.049	0.051
b-tagging efficiency for b-jets	0.003	0.016	0.023
b-tagging efficiency for c-jets	0.010	0.038	0.091
b-tagging efficiency for light jets	0.009	0.065	0.125
$E_{\mathrm{T}}^{\mathrm{miss}}$	0.001	0.003	0.008
Total systematic uncertainty	0.056	0.150	0.208
Signal statistical uncertainty	0.017	0.012	0.008
Total statistical uncertainty	0.064	0.067	0.058
Total uncertainty	0.079	0.162	0.217

WH(→WW)

ATLAS-CONF-2022-033

- Main background contribution :
  - SM diboson/triboson (dedicated CRs to constrain the background normalization)
  - Non-prompt
  - Charged-flipped
  - Photon conversion

estimated with data-driven method

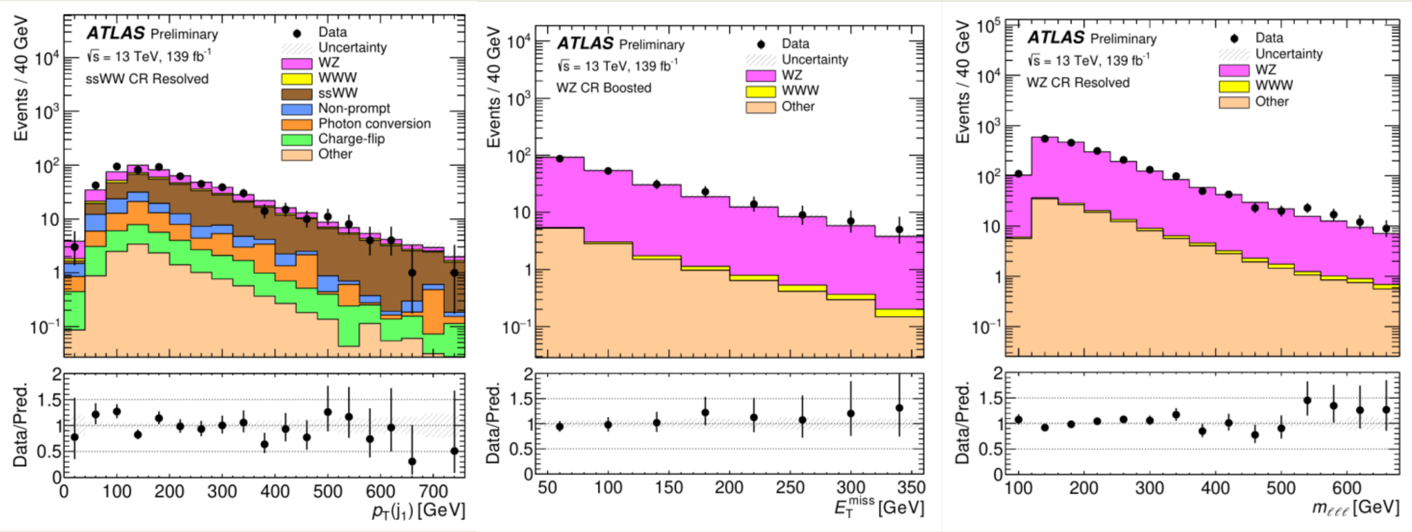

- Maximum-likelihood fits are performed on the observed binned distributions of the **"effective mass" m_{eff} discriminants** in the two SRs and CRs simultaneously.

$$m_{\text{eff}} \equiv \sum_i p_{\mathrm{T}}^i(\text{lepton}) + p_{\mathrm{T}}(\text{leading J}) + E_{\mathrm{T}}^{\text{miss}}, \quad \text{boosted category}$$

$$m_{\text{eff}} \equiv \sum_i p_{\mathrm{T}}^i(\text{lepton}) + p_{\mathrm{T}}(\text{leading j}) + p_{\mathrm{T}}(\text{sub-leading j}) + E_{\mathrm{T}}^{\text{miss}}, \quad \text{resolved category.}$$

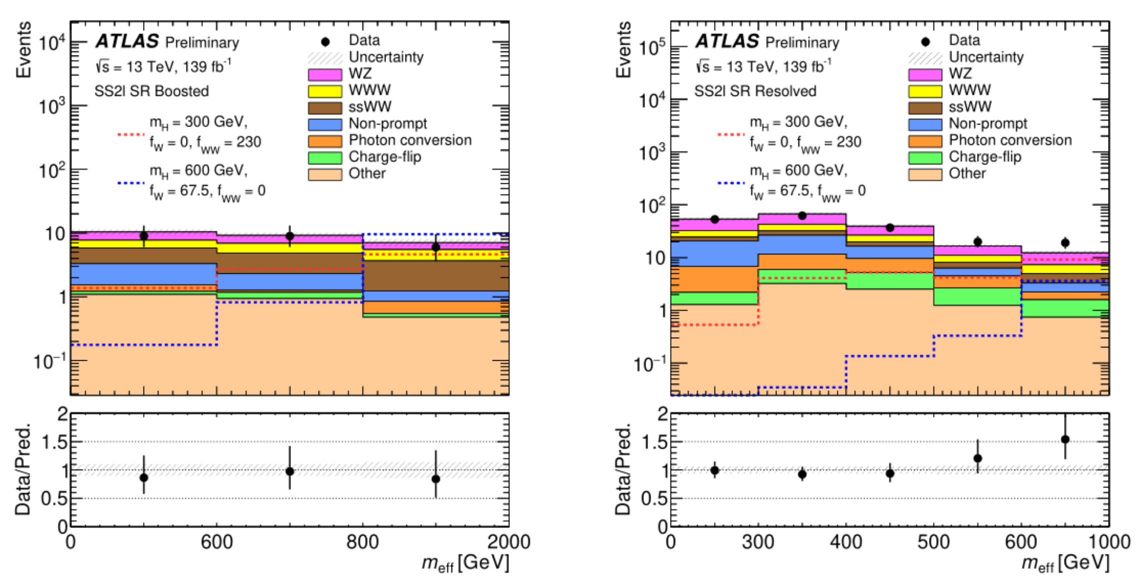

WH(→WW)

ATLAS-CONF-2022-033

- The total theoretical uncertainty in the yields from different signal samples varies between 10% and 40% in the SRs.
- The total variation on charge-flip background yields from systematic uncertainties is approximately 10%, which is dominated by the uncertainty from using directly the Z + jets MC simulation.
- The overall systematic uncertainty amounts to approximately 13% (10%) for the electron (muon) fake factors, with the dominant contribution coming from the fake factor derivations in the inclusive pT and $|\eta|$ region.
- The overall systematic uncertainty of photon conversion background is found to be approximately 8%.

Flavour-violating H→leptons+b-jets

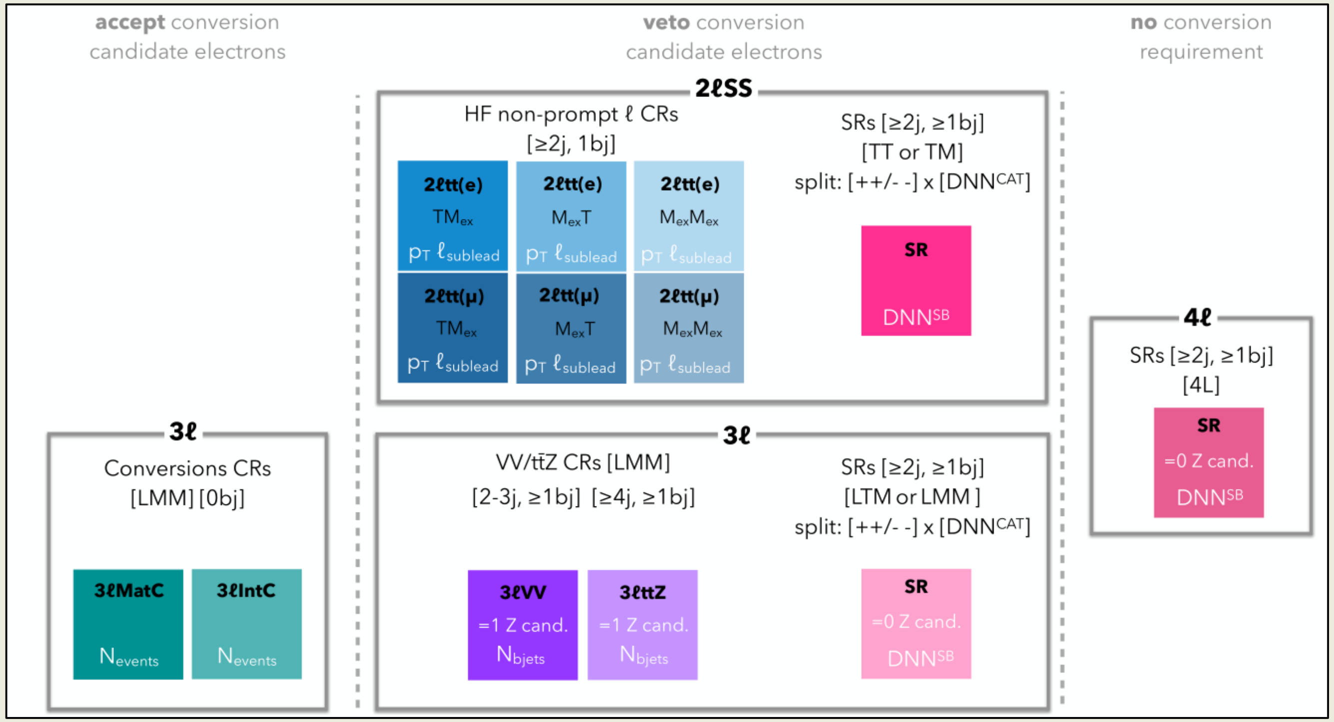

- Multiple leptons, b-jets in final states and multi-output deep neural network (DNN) classifier (DNN^{CAT}) ➔ 17 SRs + 10 CRs.
- A second DNN is trained in each of the signal regions to discriminate the signal from the total backgrounds (DNN^{SB}).

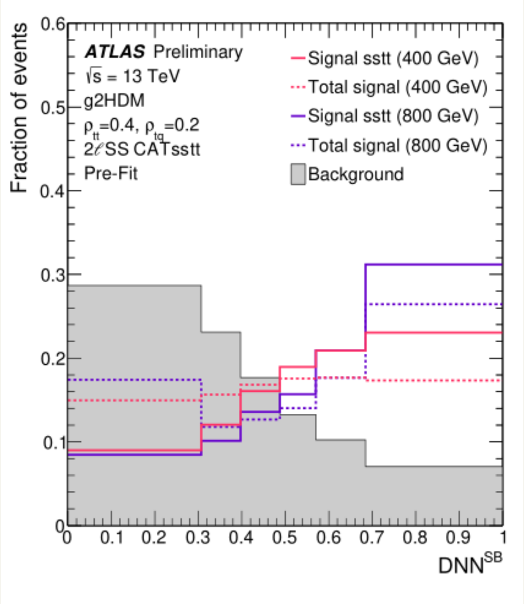

Flavour-violating H→leptons+b-jets

ATLAS-CONF-2022-039

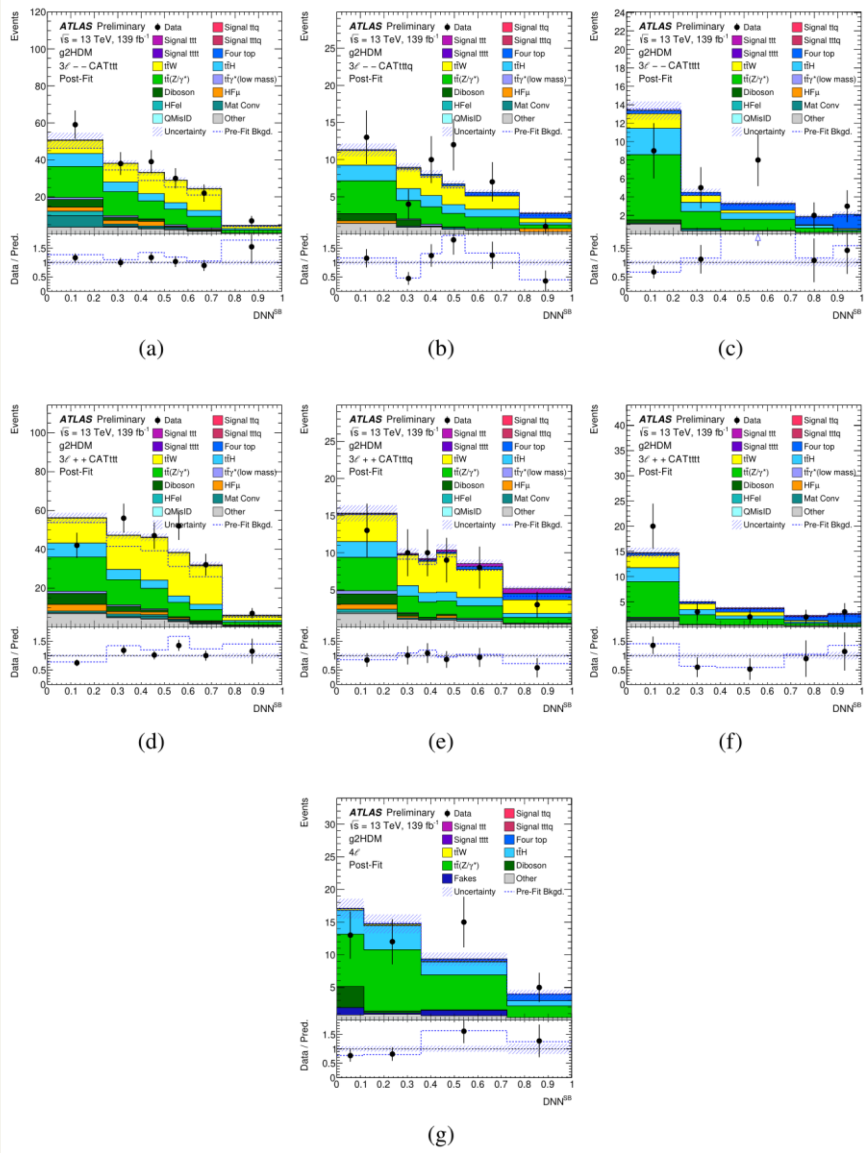

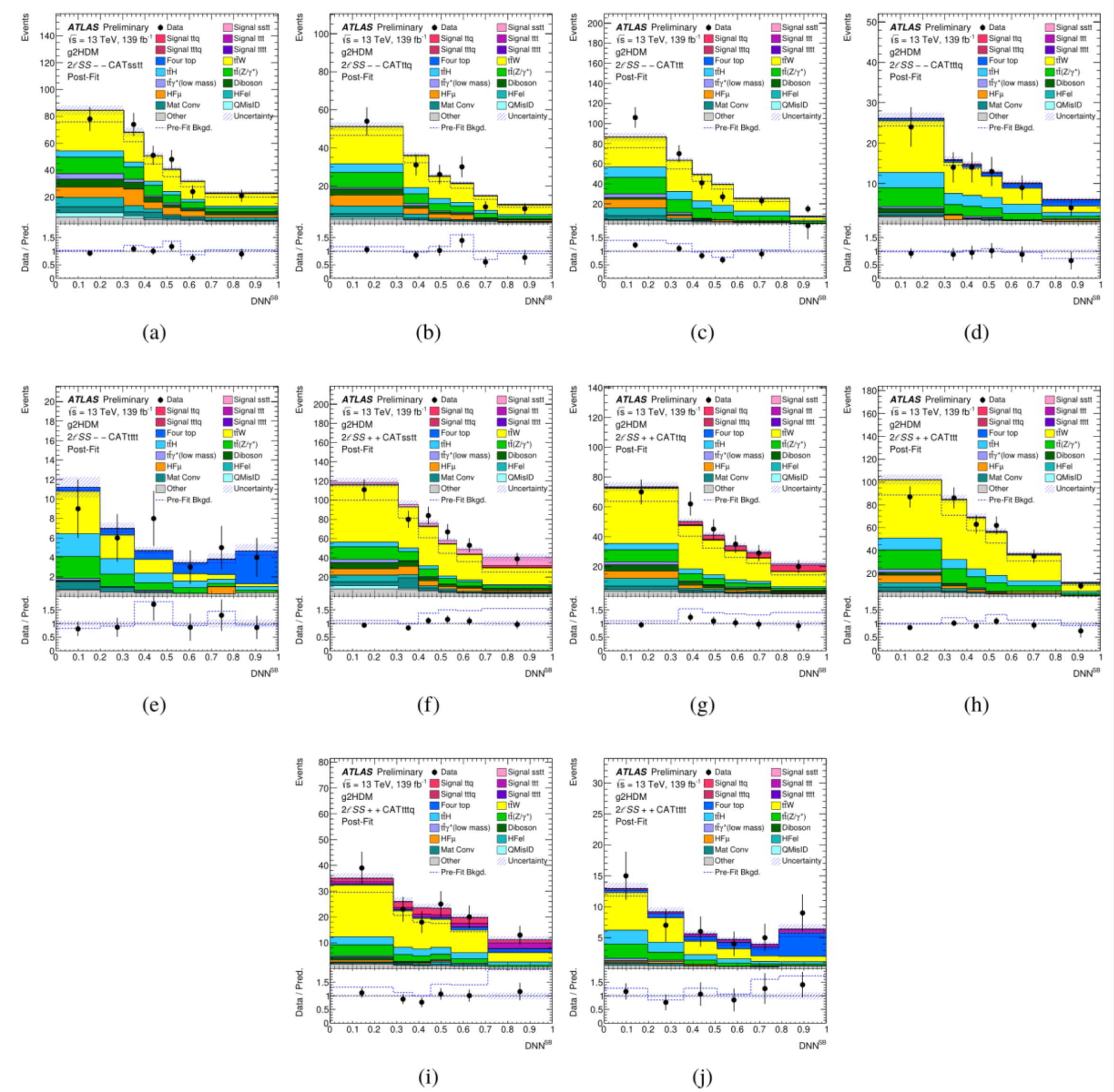

Flavour-violating H→leptons+b-jets

ATLAS-CONF-2022-039

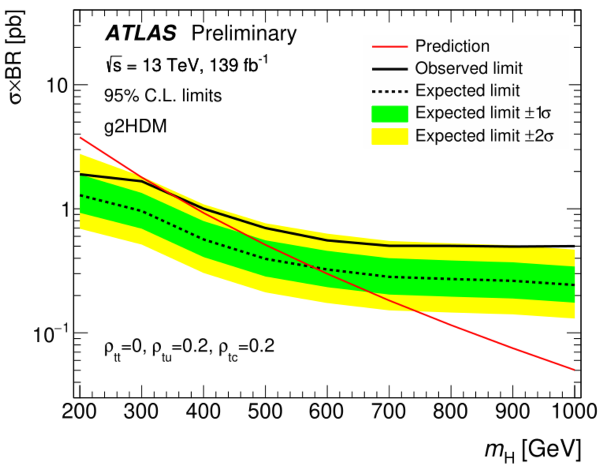

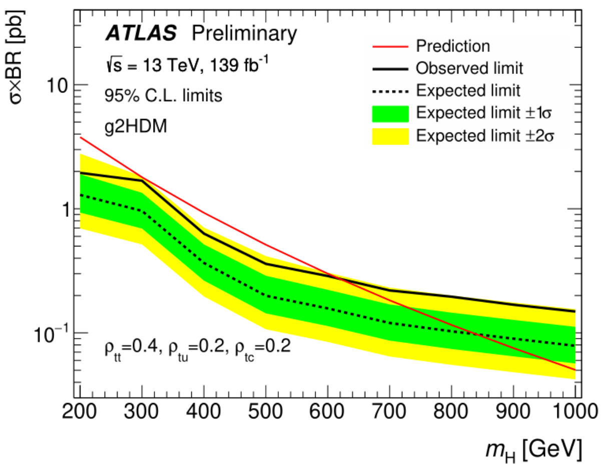

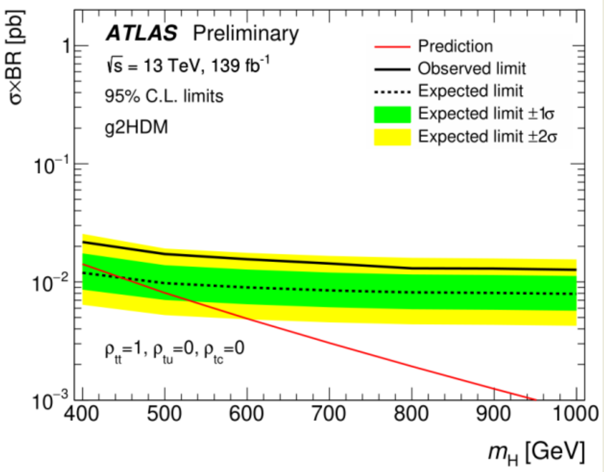

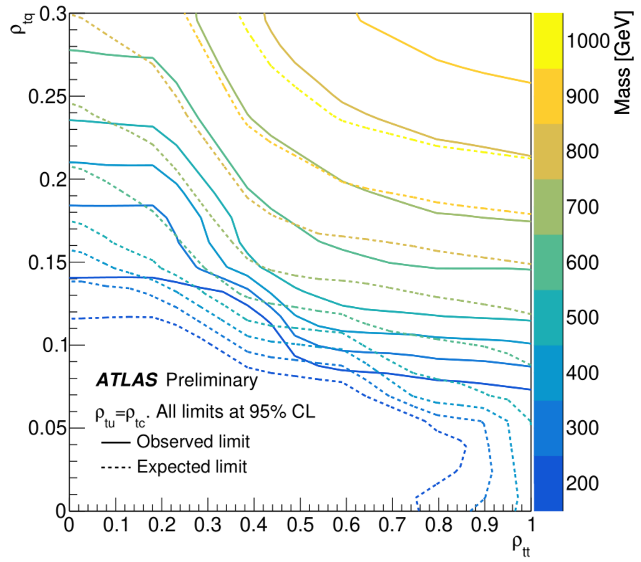

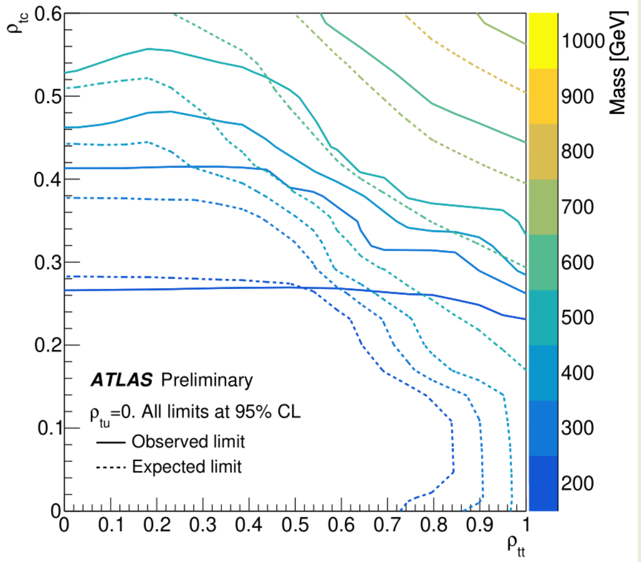

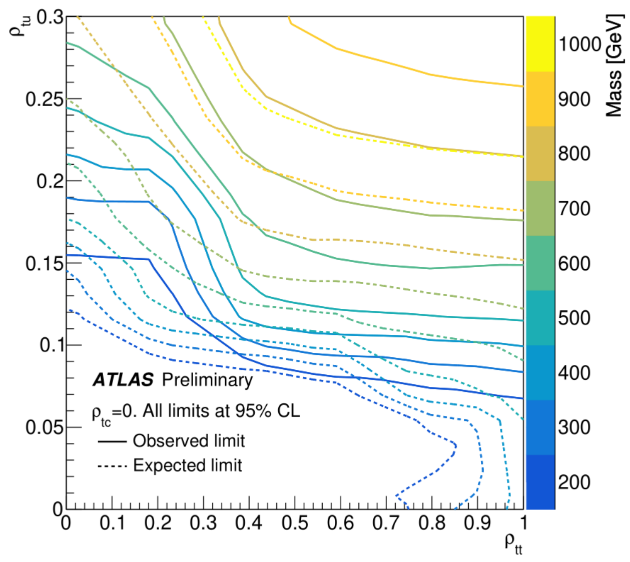

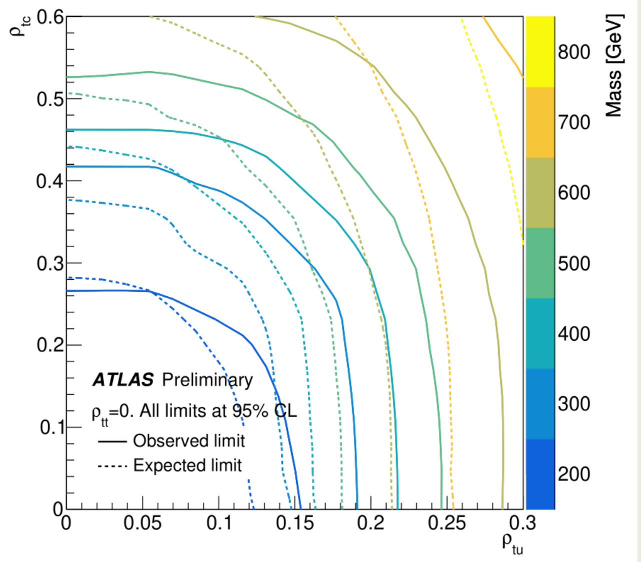

Flavour-violating H→leptons+b-jets

ATLAS-CONF-2022-039

Systematic uncertainty	Components
Signal modelling	
Cross section (N)	1
$t\bar{t}W$ modelling	
QCD scale	3
Generator	2
Electroweak cross section	1
Additional heavy-flavour	1
$t\bar{t}Z/\gamma^*$ (high mass) modelling	
QCD scale	2
Generator	2
Additional heavy-flavour	1
$t\bar{t}H$ modelling	
Cross section (N)	1
Parton shower and hadronisation model	1
Generator	1
QCD scale	1
Additional heavy-flavour	1
WZ modelling	
QCD scale	1
Cross section (N)	1
Extra-jets correction	1
$t\bar{t}t\bar{t}$ modelling	
Generator	1
Cross section (N)	1
Other background modelling	
Cross section (N)	6
Total (Signal and background modelling)	29
Luminosity	1
Pile-up reweighting	1
Physics objects	
Electron	6
Muon	15
Electron Non-prompt BDT	14
Muon Non-prompt BDT	20
Jet energy scale	30
Jet energy resolution	12
Jet vertex fraction	1
Jet flavour tagging	62
$E_{\mathrm{T}}^{\mathrm{miss}}$	3
Total (Experimental)	165
Data-driven reducible background estimates	
Material conversions modelling	1
Internal conversions modelling	1
Charge misassignment	1
HF non-prompt	8
$t\bar{t}$ additional heavy-flavour	2
Total (Data-driven reducible background)	13
Total (Overall)	207

- Additional uncertainties are evaluated from renormalization and factorisation scale variations by a factor of 0.5 and 2, relative to the nominal scales, for $t\bar{t}W$, $t\bar{t}Z$, and diboson.
- An additional 50% uncertainty is assigned to $t\bar{t}W$, $t\bar{t}Z$, and $t\bar{t}$ events with additional heavy-flavour jets.
- The $t\bar{t}t\bar{t}$, $t\bar{t}H$, and tZ processes are assigned an uncertainty of 20%, 11%, and 5%.
- A 50% cross section uncertainty is assigned as a conservative estimate to $t\bar{t}t$, tWZ, $t\bar{t}WW$, triboson backgrounds and $t\bar{t}W$ electroweak contribution.
- An uncertainty of 20% on the extrapolation from Mex to T leptons is applied.
- An additional 50% uncertainty is assigned to events originating from $t\bar{t}$ +≥ 1b and $t\bar{t}$ +≥ 1c, decorrelated between flavours.
- An $N_{b\text{-jets}}$-dependent uncertainty is added to the HF non-prompt background ranging from 6%–40% for 1–3 additional b-jets in the non-prompt muon regions, and 10%–80% in the non-prompt electron regions.

- An additional uncertainty of 10% and 50% is assigned to the material and internal conversion backgrounds.
- A systematic uncertainty of 10–60% is assigned to the background from electrons with misidentified charge.

* $A \rightarrow Zh(\rightarrow b\bar{b})$

arXiv:2207.00230

- Use transverse mass as discriminating variables: $\boldsymbol{m_{T,Zh}}$ in 0ℓ channel; $\boldsymbol{m_{Zh}}$ in 2ℓ channel.

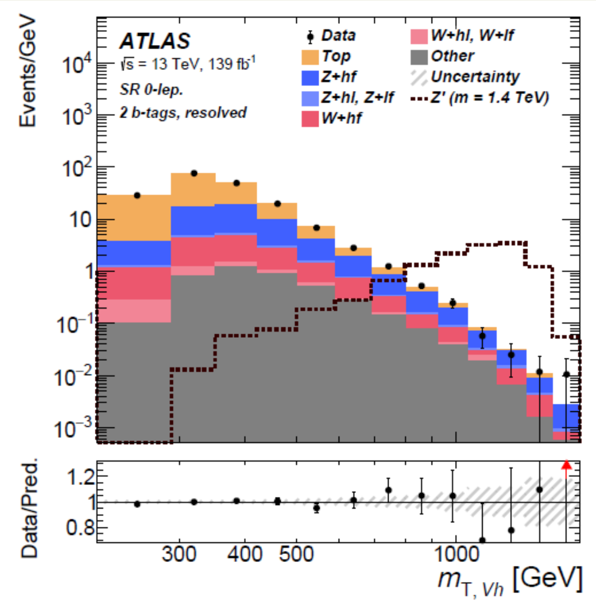

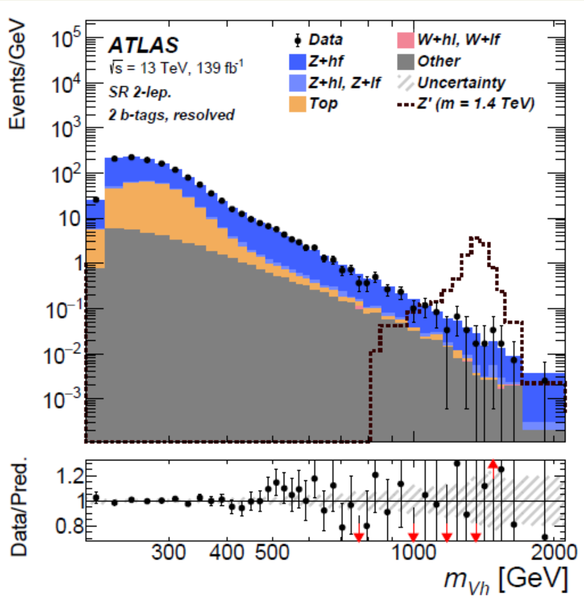

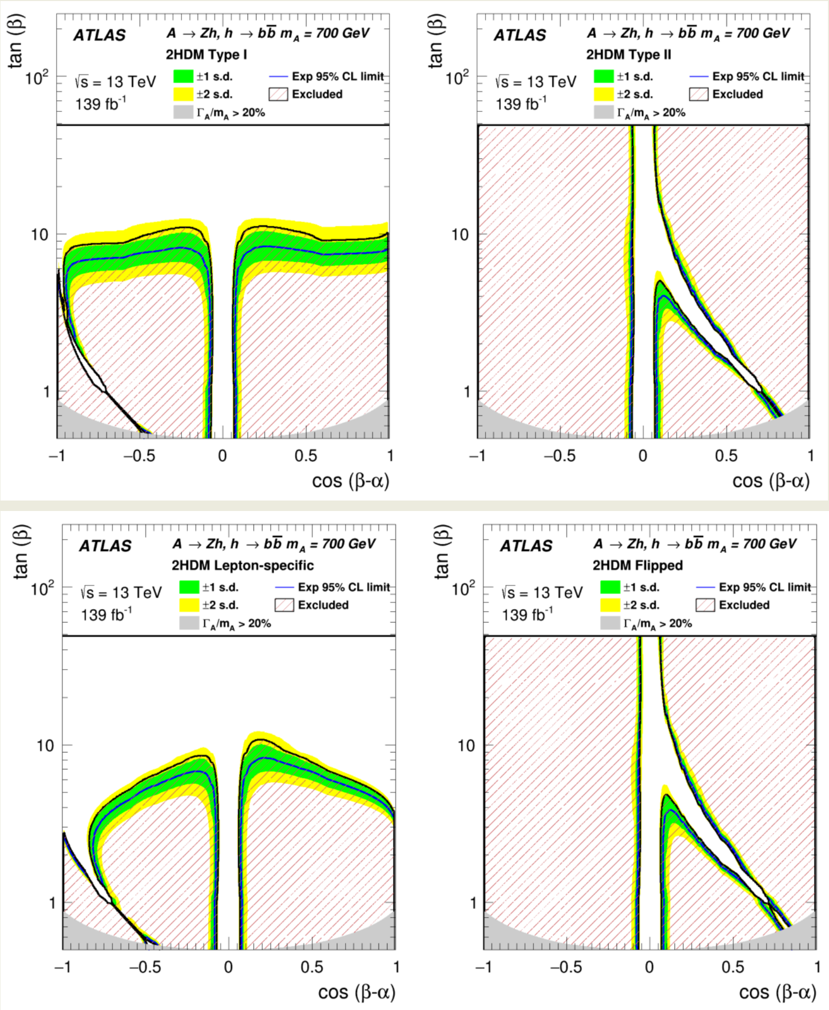

* $A \to Zh(\to b\bar{b})$

arXiv:2207.00230

Process	Quantity/source	Value
Z + hf	0/2 lep. norm.	float
	1-lep. norm.	50%
	0/2-lep. resolved ↔ merged	10%–19%
	1-lep. resolved ↔ merged	9%–18%
	0-lep. SR ↔ CR	5%–12%
	1-lep. SR ↔ CR	6%–20%
	0-lep. ↔ 1-lep.	7%–27%
	0-lep. ↔ 2-lep.	4%–16%
	generator, PDF, scale	S
	$p_{\mathrm{T},jj}$ reweighting	S
	$p_{\mathrm{T}}^{\mathrm{miss}}$ non-closure (0-lep.)	S
	$p_{\mathrm{T},W}$ non-closure (1-lep.)	S
	Large-R jet p_{T} non-closure	S
Z + hl	0/2 lep. norm.	float
	1-lep. norm.	50%
	0/2 lep. resolved ↔ merged	15%–28%
	1-lep. resolved ↔ merged	12%–13%
	0-lep. SR ↔ CR	3%–20%
	1-lep. SR ↔ CR	5%–7%
	0-lep. ↔ 1-lep.	7%–27%
	0-lep. ↔ 2-lep.	6%–17%
	generator, PDF, scale	S
	$p_{\mathrm{T},jj}$ reweighting	S
	$p_{\mathrm{T}}^{\mathrm{miss}}$ non-closure (0-lep.)	S
	$p_{\mathrm{T},W}$ non-closure (1-lep.)	S
	Large-R jet p_{T} non-closure	S
Z + lf	norm.	19%
	0/2 lep. resolved ↔ merged	8%–50%
	1-lep. resolved ↔ merged	10%–29%
	0-lep. SR ↔ CR	5%–20%
	1-lep. SR ↔ CR	29%–99%
	0-lep. ↔ 1-lep.	8%–39%
	0-lep. ↔ 2-lep.	4%–17%
	generator, PDF, scale	S
	$p_{\mathrm{T},jj}$ reweighting	S
	$p_{\mathrm{T}}^{\mathrm{miss}}$ non-closure (0-lep.)	S
	$p_{\mathrm{T},W}$ non-closure (1-lep.)	S
	Large-R jet p_{T} non-closure	S

Process	Quantity/source	Value
W + hf	0/2 lep. norm.	30%
	1-lep. norm.	float
	0/2 lep. resolved ↔ merged	13%–28%
	1-lep. resolved ↔ merged	15%–22%
	0-lep. SR ↔ CR	5%–28%
	1-lep. SR ↔ CR	3%
	0-lep. ↔ 1-lep.	4%
	generator, PDF, scale	S
	$p_{\mathrm{T},jj}$ reweighting (0-lep.)	S
	$p_{\mathrm{T}}^{\mathrm{miss}}$ non-closure (0-lep.)	S
	$p_{\mathrm{T},W}$ non-closure (1-lep.)	S
	Large-R jet p_{T} non-closure	S
	JetBinMigration (1-lep.)	S
W + hl	0/2 lep. norm.	30%
	1-lep. norm.	float
	0/2 lep. resolved ↔ merged	2%–43%
	1-lep. resolved ↔ merged	12%–13%
	0-lep. SR ↔ CR	2%–20%
	1-lep. SR ↔ CR	1%–2%
	0-lep. ↔ 1-lep.	4%
	generator, PDF, scale	S
	$p_{\mathrm{T},jj}$ reweighting (0-lep.)	S
	$p_{\mathrm{T}}^{\mathrm{miss}}$ non-closure (0-lep.)	S
	$p_{\mathrm{T},W}$ non-closure (1-lep.)	S
	Large-R jet p_{T} non-closure	S
	JetBinMigration (1-lep.)	S
W + lf	0/2 lep. norm.	20%
	1-lep. norm.	float
	0/2 lep. resolved ↔ merged	14%–18%
	1-lep. resolved ↔ merged	20%–21%
	0-lep. SR ↔ CR	4%–20%
	1-lep. SR ↔ CR	2%–4%
	generator, PDF, scale	S
	$p_{\mathrm{T},jj}$ reweighting (0-lep.)	S
	$p_{\mathrm{T}}^{\mathrm{miss}}$ non-closure (0-lep.)	S
	$p_{\mathrm{T},W}$ non-closure (1-lep.)	S
	Large-R jet p_{T} non-closure	S
	JetBinMigration (1-lep.)	S

Process	Quantity/source	Value
Signal	PS, ISR/FSR, PDF	2%–7%, S
SM Vh	0/1/2-lep norm.	32%
	$p_{\mathrm{T}}^{\mathrm{miss}}$ non-closure (0-lep.)	S
	$p_{\mathrm{T},W}$ non-closure (1-lep.)	S
	Large-R jet p_{T} non-closure	S
Diboson	0/1-lep norm.	50%
	2-lep norm.	20%
	$p_{\mathrm{T}}^{\mathrm{miss}}$ non-closure (0-lep.)	S
	$p_{\mathrm{T},W}$ non-closure (1-lep.)	S
	Large-R jet p_{T} non-closure	S

Process	Quantity/source	Value
Top quark	0/1/2-lep. norm. ($b\bar{b}A$: separate $t\bar{t}$ +hf norm.)	float
	single-top-quark contribution	19%
	$t\bar{t}+V$ contribution	50%
	$t\bar{t}+h$ contribution	50%
	0-lep. resolved ↔ merged	9%–20%
	1-lep. resolved ↔ merged	18%–20%
	2-lep. resolved ↔ merged	18%
	0-lep. SR ↔ CR	2%–12%
	1-lep. SR ↔ CR	2%–3%
	2-lep. SR ↔ CR	1.2%
	PS, ISR/FSR, ME, PDF	S
	DS vs DR scheme (Wt)	S
	$p_{\mathrm{T}}^{\mathrm{miss}}$ non-closure (0-lep.)	S
	$p_{\mathrm{T},W}$ non-closure (1-lep.)	S
	Large-R jet p_{T} non-closure	S

* VH(→hh)

[ATLAS-CONF-2022-043]

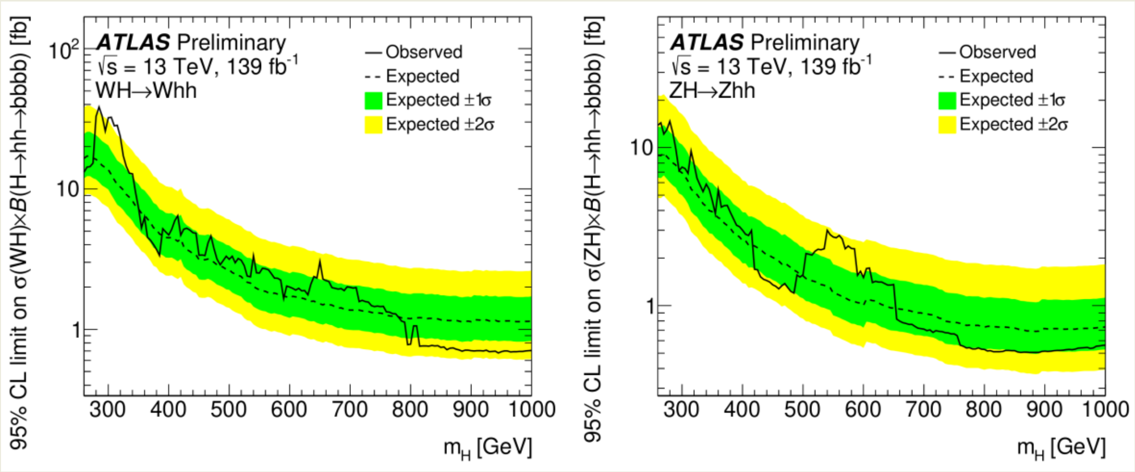

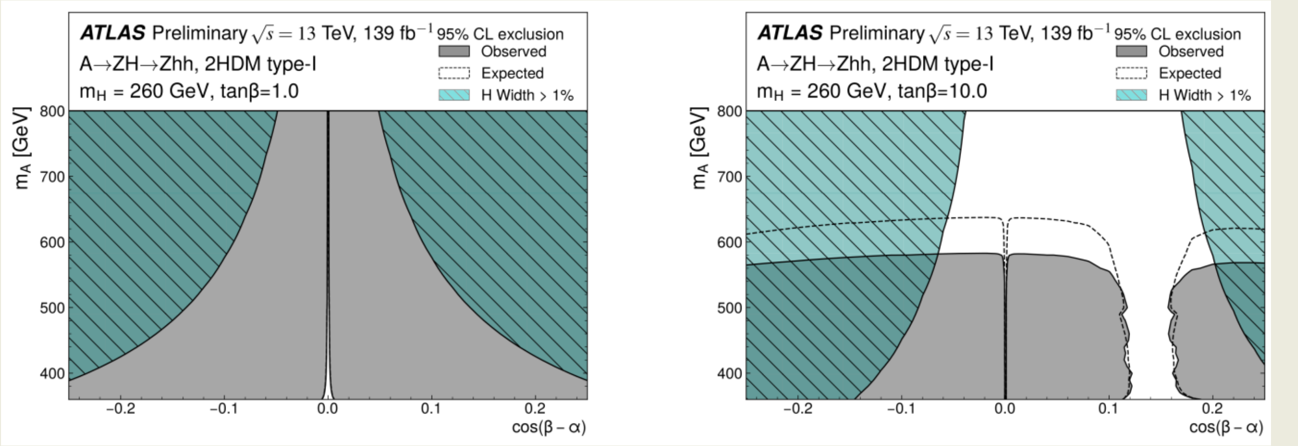

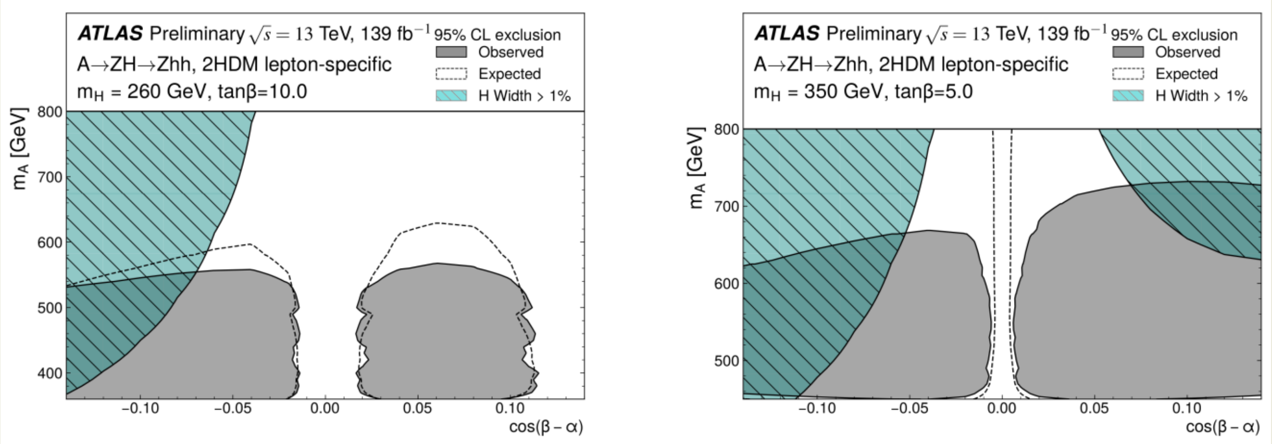

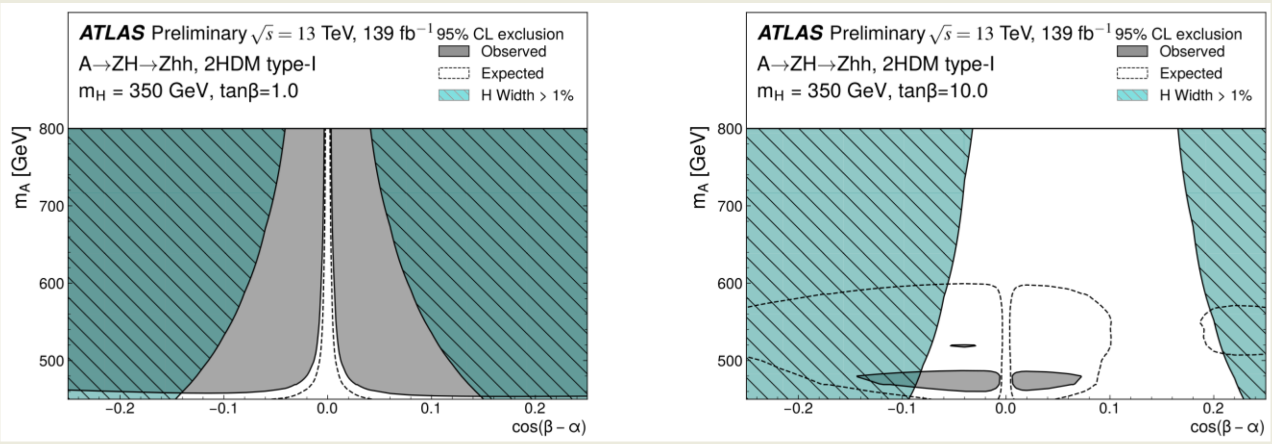

* VH(→hh)

ATLAS-CONF-2022-043

Model	SM-like Vhh	WH	ZH	NW $A \to ZH$	LW $A \to ZH$
Systematic uncertainty source			$\Delta\mu/\mu$ [%]		
Background modelling	+20, −15	+14, −11	+4.7, −3.0	+16, −12	+20, −18
MC statistics	+12, −9.1	+13, −7.8	+4.8, −2.2	+6.6, −3.9	+10, −8.3
Objects	+12, −8.6	+8.0, −5.2	+4.5, −2.2	+19, −11	+16, −12
Signal modelling	+10, −4.7	+12, −4.9	+8.6, −3.0	+13, −5.4	+17, −7.6
VR non-closure	+14, −11	+11, −9.4	+4.4, −3.0	+4.2, −3.3	+12, −10
Total systematic	+30, −22	+27, −18	+12, −5.8	+27, −16	+33, −24
Statistical	+44, −39	+52, −43	+68, −49	+53, −42	+42, −37
Total	+52, −44	+59, −47	+69, −49	+60, −46	+53, −45

Low mass $X \to \gamma\gamma$

[ATLAS-CONF-2022-018]

- The turn-on region (TO) is described by an exponential function: $h_{\mathrm{TO}}(m_{\gamma\gamma}; f_0, \tau_{\mathrm{TO}}) = 1 - (1 - f_0)e^{-\frac{m_{\gamma\gamma}}{\tau_{\mathrm{TO}}}}$
- The smoothly falling region beyond 30 GeV is described by a power-law functional form multiplied by an "activation" function, to increase its flexibility in the high mass region (above 50 GeV).
- The total function is given by:

$$h_{\mathrm{High}}(m_{\gamma\gamma}; c_1, a_0, c_0, \delta_{\mathrm{tail}}, \tau_{\mathrm{tail}}, \delta_{\mathrm{thresh}}, \tau_{\mathrm{thresh}}) = \underbrace{\left(1 - \left(\frac{m_{\gamma\gamma}}{c_1}\right)^{a_0}\right)^{c_0}}_{\text{Power-law}} \underbrace{\left(1 + \frac{e^{\frac{m_{\gamma\gamma}-\delta_{\mathrm{tail}}}{\tau_{\mathrm{tail}}}}}{1 + e^{-\frac{m_{\gamma\gamma}-\delta_{\mathrm{thresh}}}{\tau_{\mathrm{thresh}}}}}\right)}_{\text{Activation function}}$$

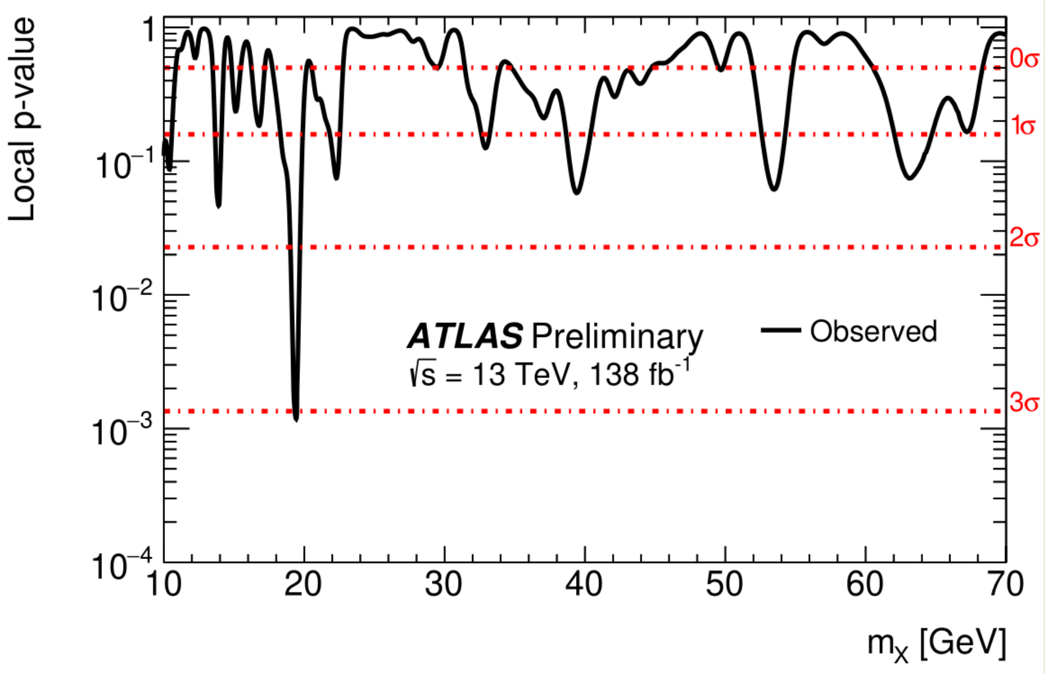

Source	Uncertainty
	On $\sigma_{\mathrm{fid}} \cdot \mathcal{B}(X \to \gamma\gamma)$ [%]
Pile-up modeling	± 3.5 (at 10 GeV) – ± 2 (beyond 15 GeV), mass dependent
Photon energy resolution	± 2.5 – ± 2.7, mass dependent
Scale and PDFs uncertainties	± 2.5 – ± 0.5, mass dependent
Trigger on close-by photons	±2 (at 10 GeV) – < 0.1 (beyond 35 GeV), mass dependent
Photon identification	±2.0
Isolation efficiency	±2.0
Luminosity (2015–2018)	±1.7
Trigger	±1.0
Signal shape modeling	< 1
Photon energy scale	negligible
Background modeling	
Spurious signal (relative to δS)	30-65 events (10-30 %), mass dependent

$H^{++}H^{--} \rightarrow 4l$

ATLAS-CONF-2022-010

- Signal regions separated by lepton multiplicities (2L, 3L, 4L).
- $\boldsymbol{m(l^{\pm}, l'^{\pm})}$ used as main discriminant.
- Simultaneous fit over the invariant mass distributions in the SR and CR of the 2L and 3L final states plus a single bin event yield in the 4L final state to obtain the number of signal and background events.
- The limit obtained from the four-lepton final state is the most sensitive and drives the combined result.

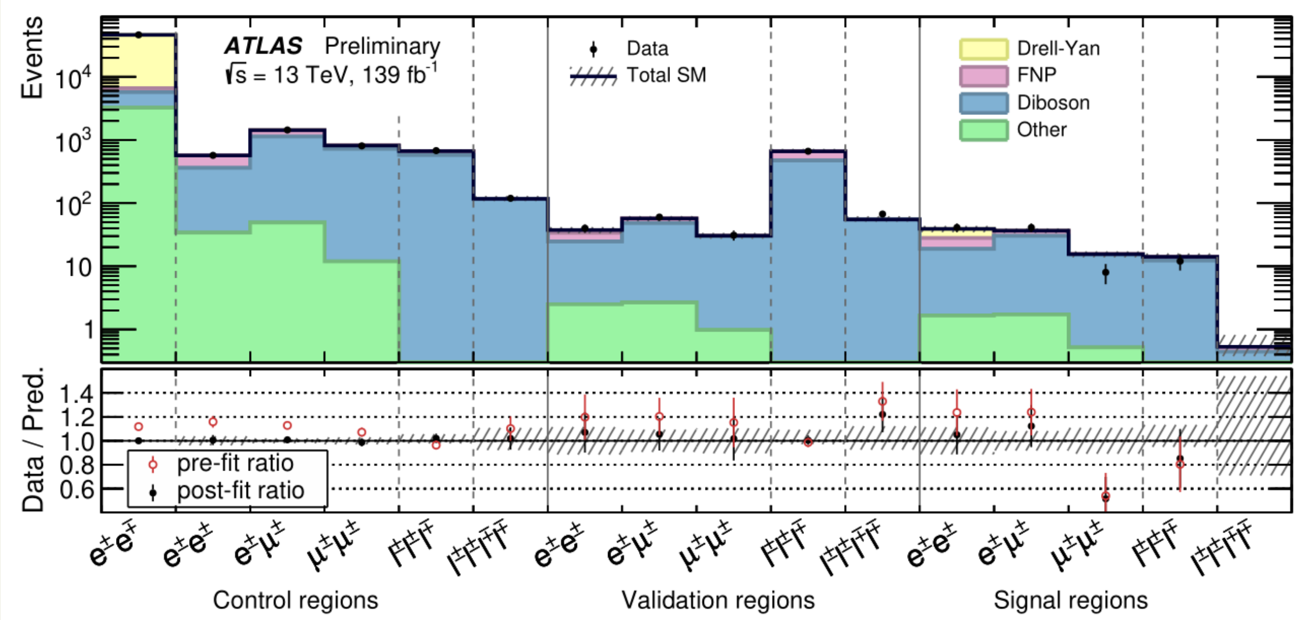

* $H^{++}H^{--} \rightarrow 4l$

ATLAS-CONF-2022-010

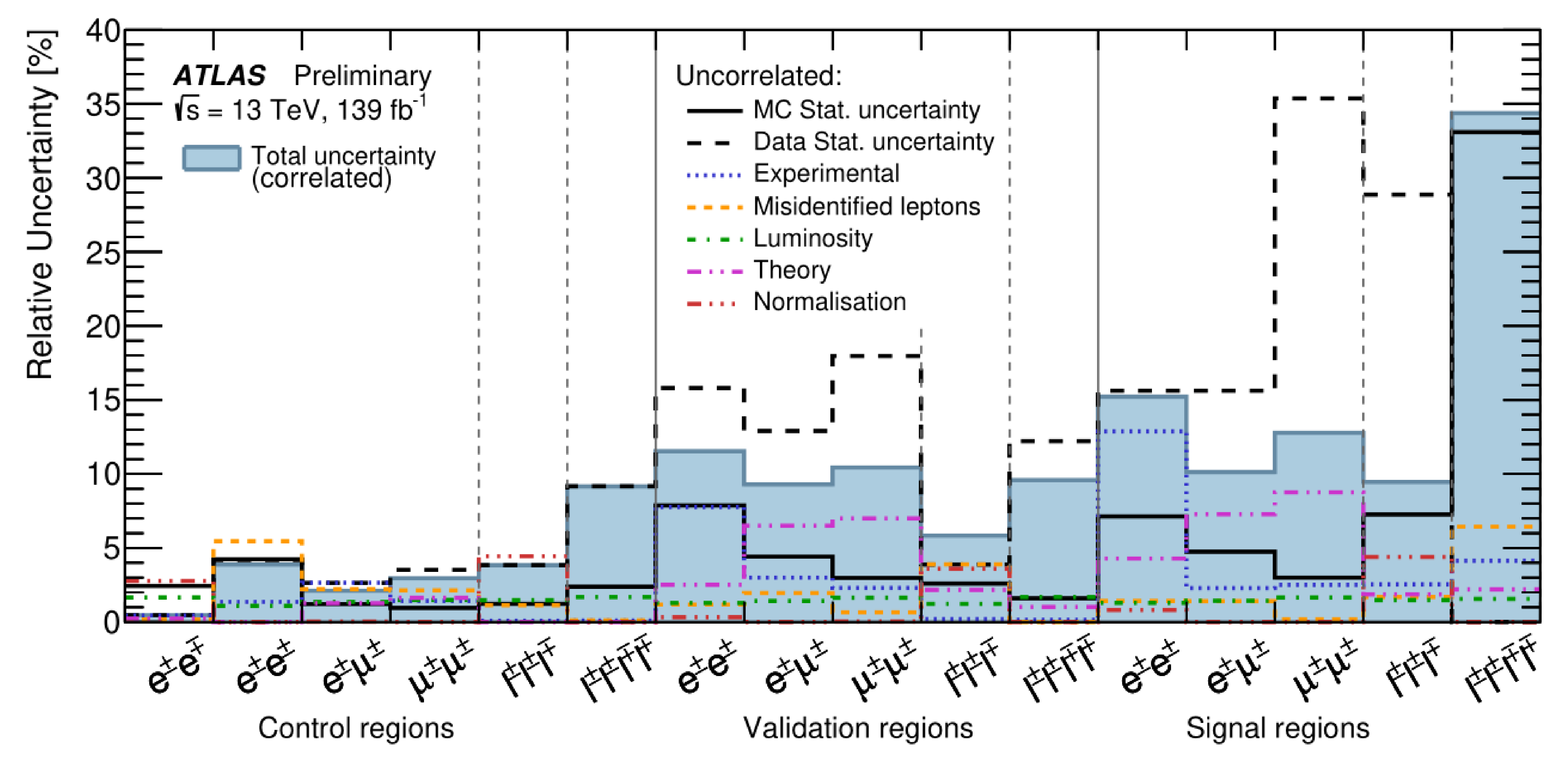

* $H^{\pm} \rightarrow ZW \rightarrow l\nu l'l'$

arXiv:2207.03925

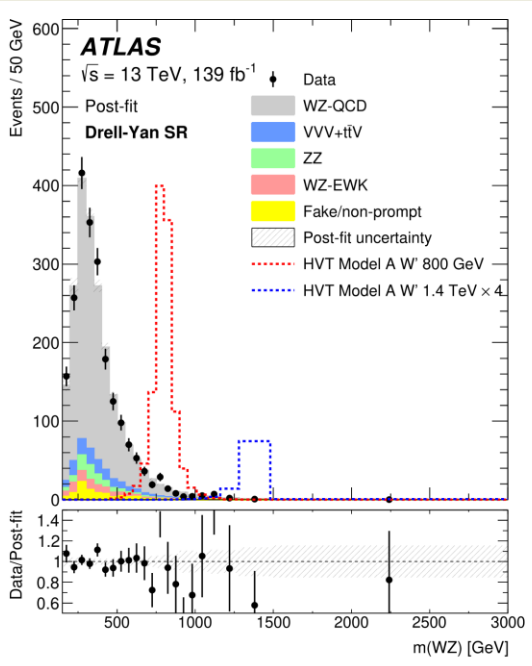

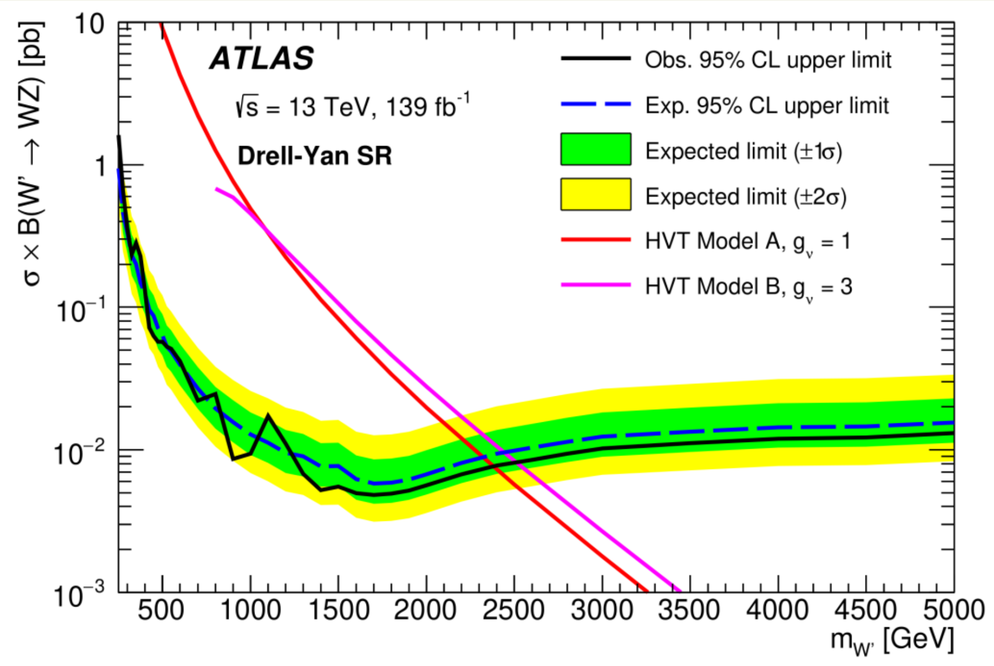

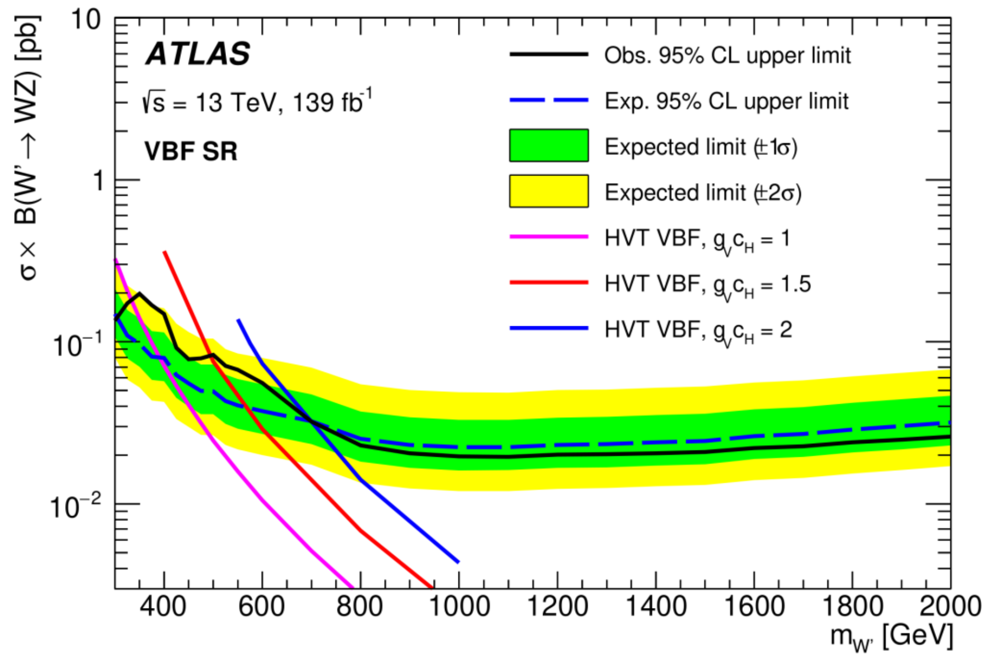

$H^{\pm} \rightarrow ZW \rightarrow l\nu l'l'$

arXiv:2207.03925

- Theory uncertainties
  - For the WZ–EWK background the uncertainties in the m(WZ) shape grow with the mass from 8% to 15%.
  - For the WZ–EWK they are added in quadrature, and the total uncertainty stays between 5 to 6% in all mass bins for both the Drell-Yan and VBF selections.
  - A modelling uncertainty in the WZ-QCD background template has no effect on the m(WZ) distribution's normalization at low mass, but grows to 5% at high mass.
  - For the ZZ background the shape uncertainties originating from the renormalization and factorization scales, as well as from the PDF and the chosen value of αs are evaluated in a similar way.
  - An uncertainty of 20% is assigned to $t\bar{}tV$ and VVV cross-sections.
  - The theory uncertainties of the HVT signals are evaluated to be less than 20% for all production modes and they are 30% for the GM model.
- Experimental uncertainties
  - The effect of jet uncertainties on the expected number of events ranges up to 15% in the VBF selection.
  - An uncertainty in the prediction of the fake/non-prompt background is about 60% (more than 100%) for the Drell–Yan (VBF) selections.

Summary plots for hMSSM interpretations

PUB–HDBS–2022–09

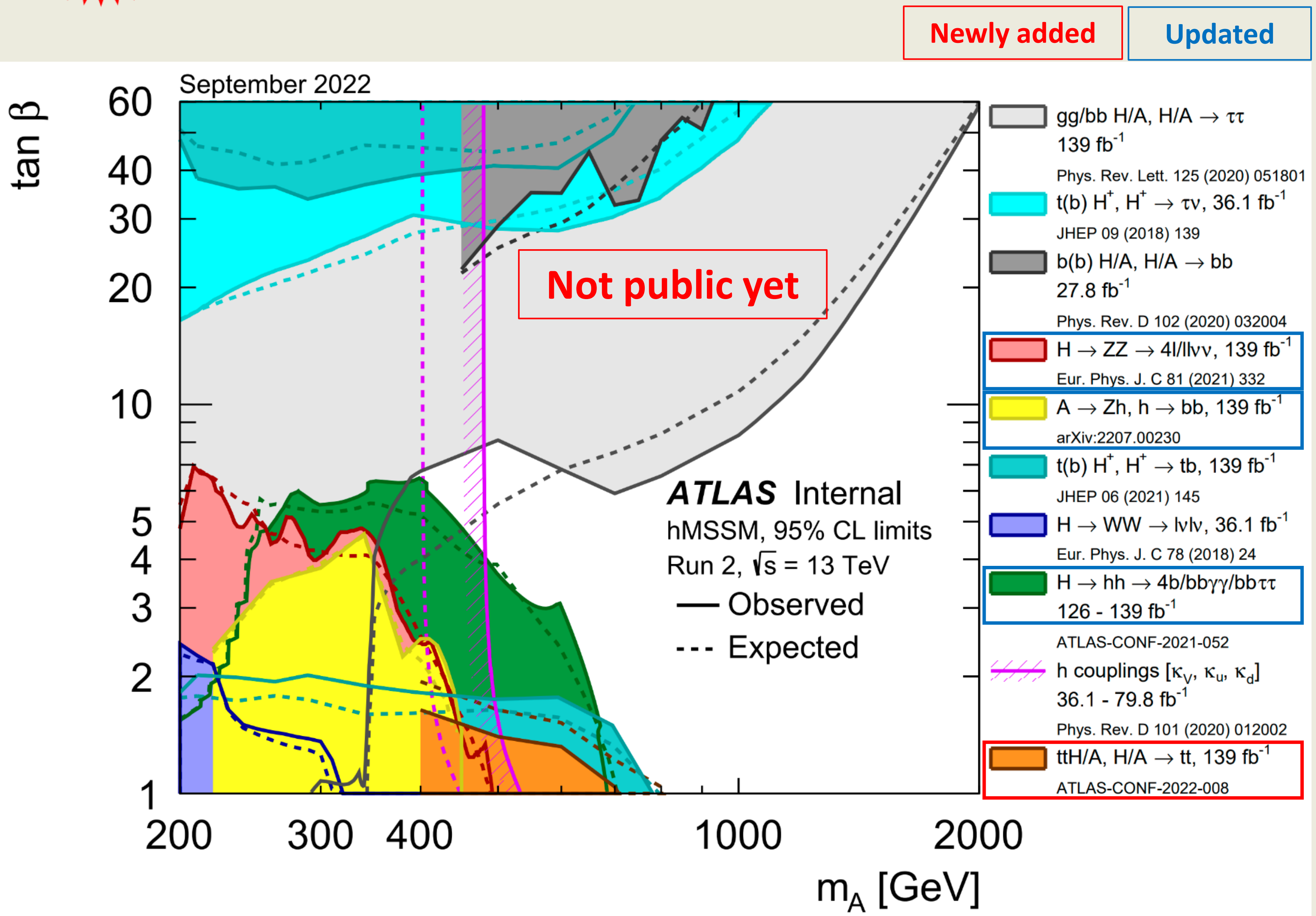

- Regions of the $[m_A, tan\beta]$ plane excluded in the hMSSM via direct searches for heavy Higgs bosons and fits to the measured rates of observed Higgs boson production and decays.
- Limits are quoted at 95% CL and are indicated for the data (solid lines) and the expectation for the SM Higgs sector (dashed lines). The light shaded or hatched regions indicate the observed exclusions.
- Unless otherwise specified, only gluon–gluon fusion is considered for the production mode.
- The cross-sections for the Higgs boson production in the hMSSM are calculated using up to NNLO QCD corrections for gluon–gluon fusion and b-associated production in the five-flavour scheme as implemented in *Sushi*. For b-associated production a cross-section in the four-flavour scheme is calculated and the results are combined with the five-flavour scheme calculation.
- The Higgs boson widths and branching ratios have been calculated using *HDECAY*.

NEW! Summary plots for Type-I 2HDM interpretations

PUB–HDBS–2022–09

The excluded regions are obtained by interpreting the ATLAS cross-section upper limits for gluon–gluon fusion produced Higgs bosons only. The large asymmetry in $H \rightarrow hh$ between $\cos(\beta - \alpha) = 0.1$ and -0.1 is mainly due to the structure of the Hhh coupling. These limits assume a narrow width Higgs boson, an assumption that is not valid for H boson widths beyond 5% due to possible interference effects. Such regions constitute large parts of the parameter space probed and they are denoted by hatched areas in the figures. For the search for Higgs boson pairs, the experimental analysis considers the combination of three channels: $bbbb$, $bb\tau\tau$ and $bb\gamma\gamma$. The $bb\gamma\gamma$ channel is sensitive to natural widths of the H boson lower than a few percent, depending on the assumed mass of the H boson, and for that reason it has only been used in those parameter space areas that the 2HDM width prediction for the H boson is compatible with the experimental analysis in this channel. This is found to coincide with the region $m_H \leq$ 600 GeV. The rest of the parameter space (m_H > 600 GeV) uses the combination of only $bbbb$ and $bb\tau\tau$ channels. For the parameter space shown in these plots there is no similar issue with the width of the A boson. The excluded parameter space from this final state evades the constraints from H boson width and this is the reason it is shown superimposed on the region in which the width of H boson is more than 5%.